Anisotropies in ultra-high energy cosmic rays

Olivier Deligny (CNRS/IN2P3 - IPN Orsay, France)

A BAM in the Anisotropic Universe—September 2018

i) Ultra-high energy cosmic rays

Ultra-high energy cosmic rays: contemporary questions

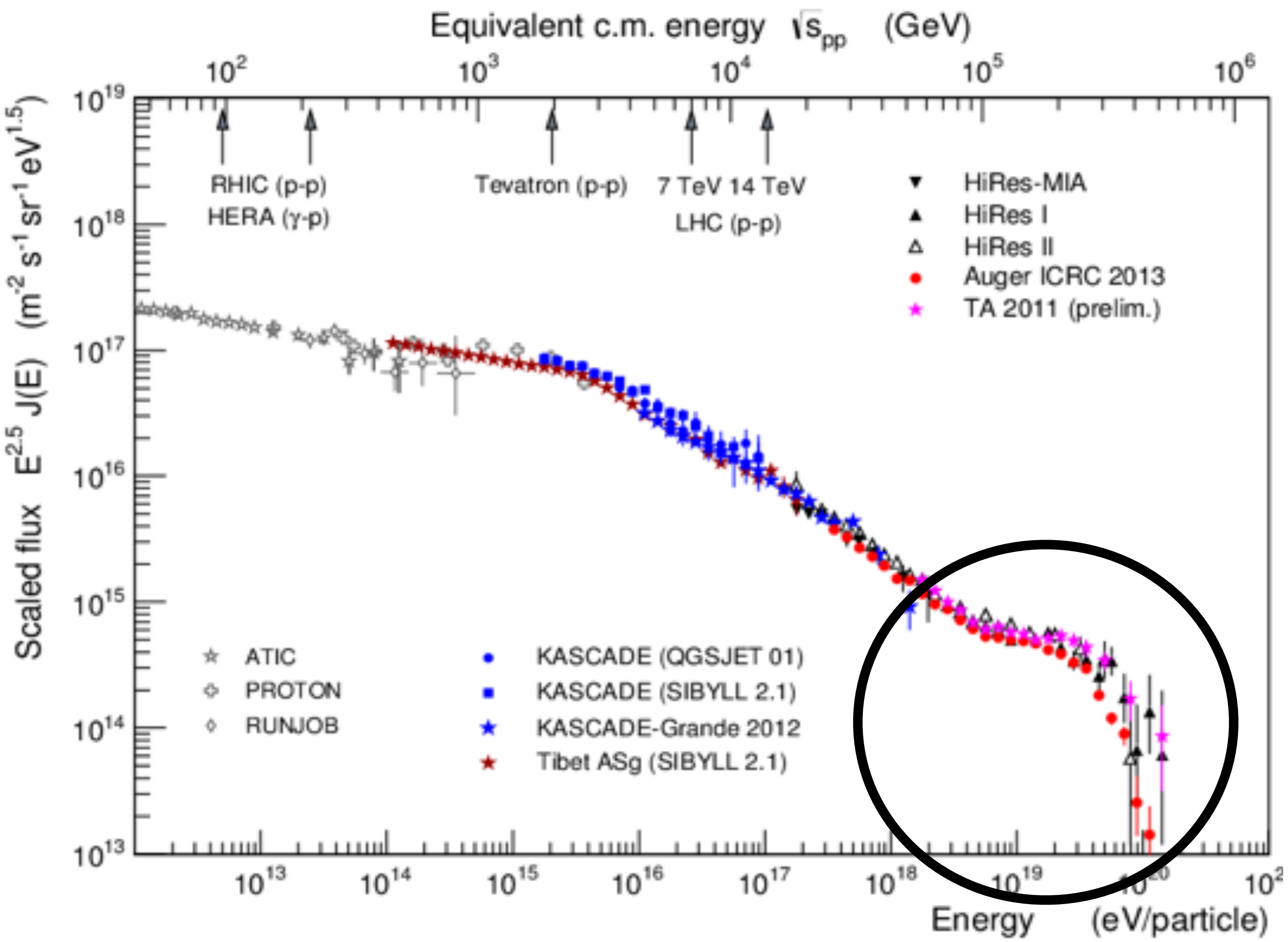

- Gal/xGal transition?
- Origin of the ankle?
- Origin of the UHE steepening?
- Composition at UHE?
- Sources?

NB: From neutrinos/photons upper limits, the bulk of UHECRs are accelerated particles in astrophysical objects

The GZK cutoff

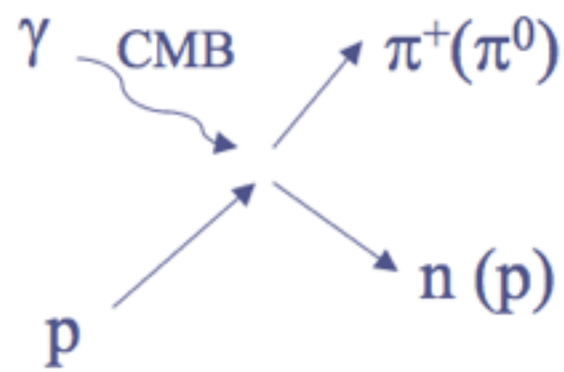

Example with protons

$$\varepsilon_\gamma > \frac{m_\pi m_p}{\varepsilon_p} \sim 10^{-3}\varepsilon_{20}^{-1}\ \mathrm{eV} \Rightarrow \quad n_\gamma \sim \frac{400}{\mathrm{cm}^3}\exp\left[1-\frac{3}{\varepsilon_{20}}\right]$$

$$\lambda_E \sim \frac{m_p}{m_\pi}\frac{1}{n_\gamma \sigma_{\gamma p}}$$

$$\sim 11\exp\left[\frac{3}{\varepsilon_{20}}-1\right] \quad \mathrm{Mpc}$$

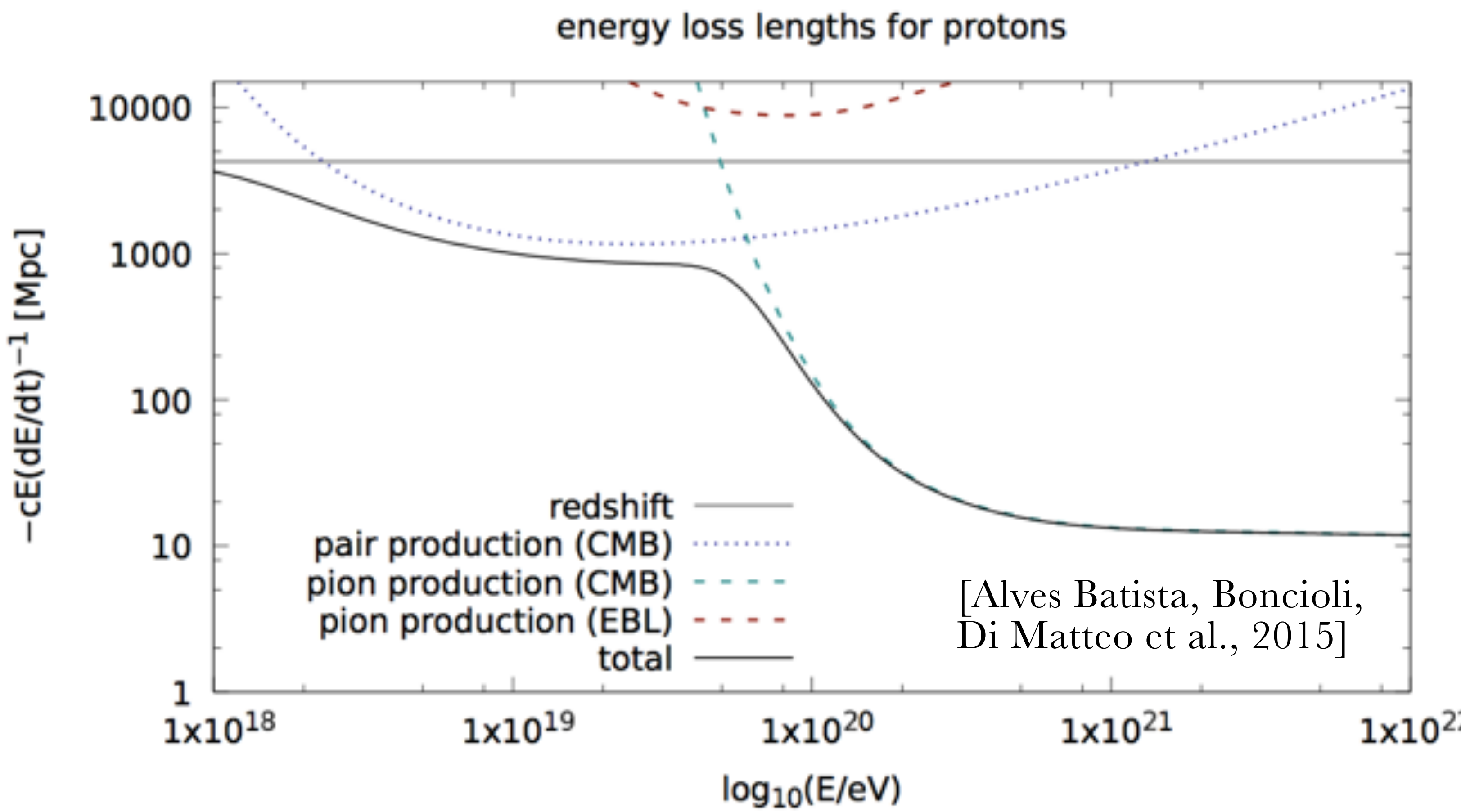

Same phenomenon with nuclei (photo-disintegration)

➡ Sudden reduction of the CR horizon at UHE

Energy spectrum/Mass composition

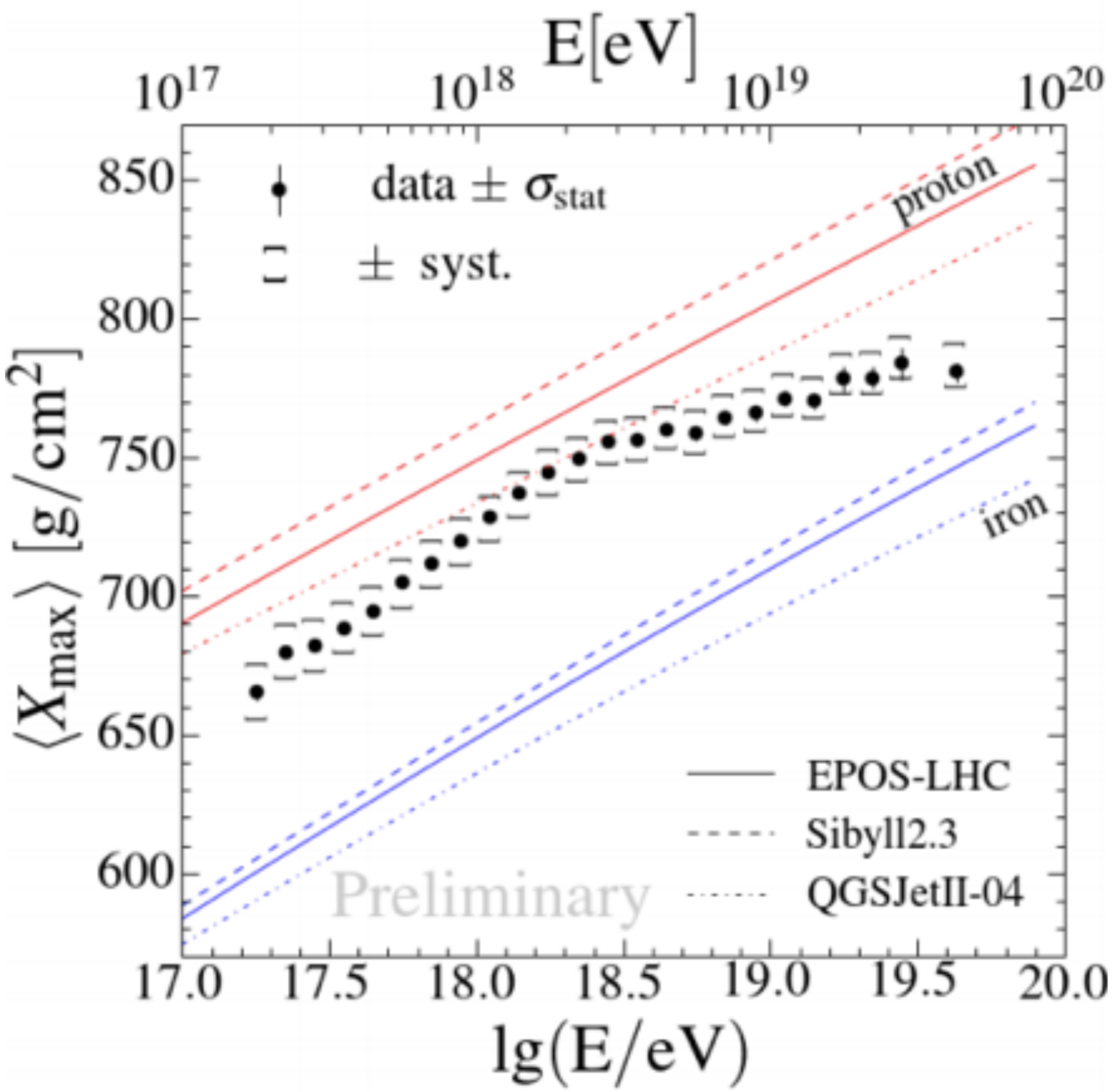

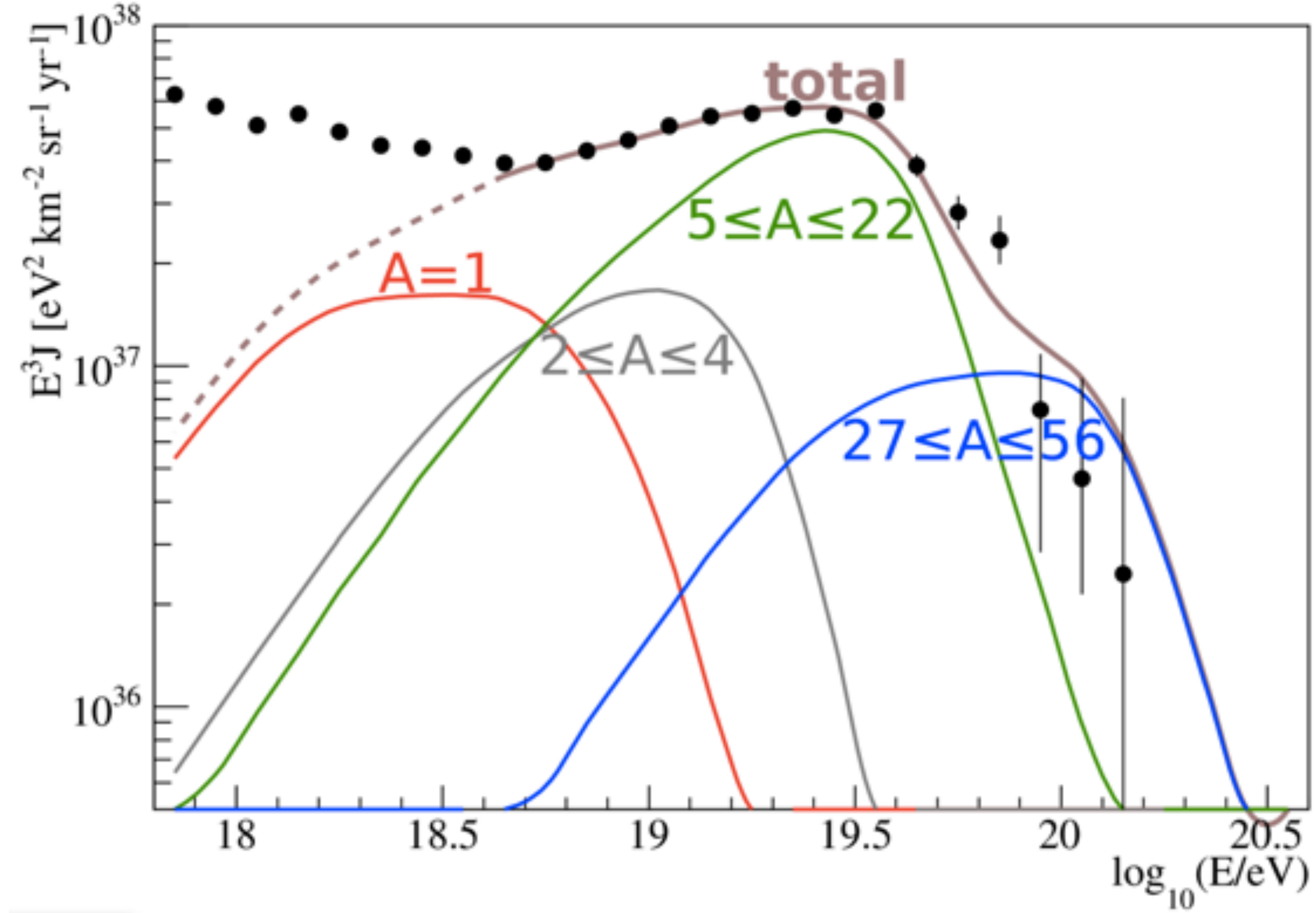

- Intermediate/heavy nuclei at ultra-high energies
- Interplay between maximum acceleration energy and GZK cutoff?

Magnetic deflections

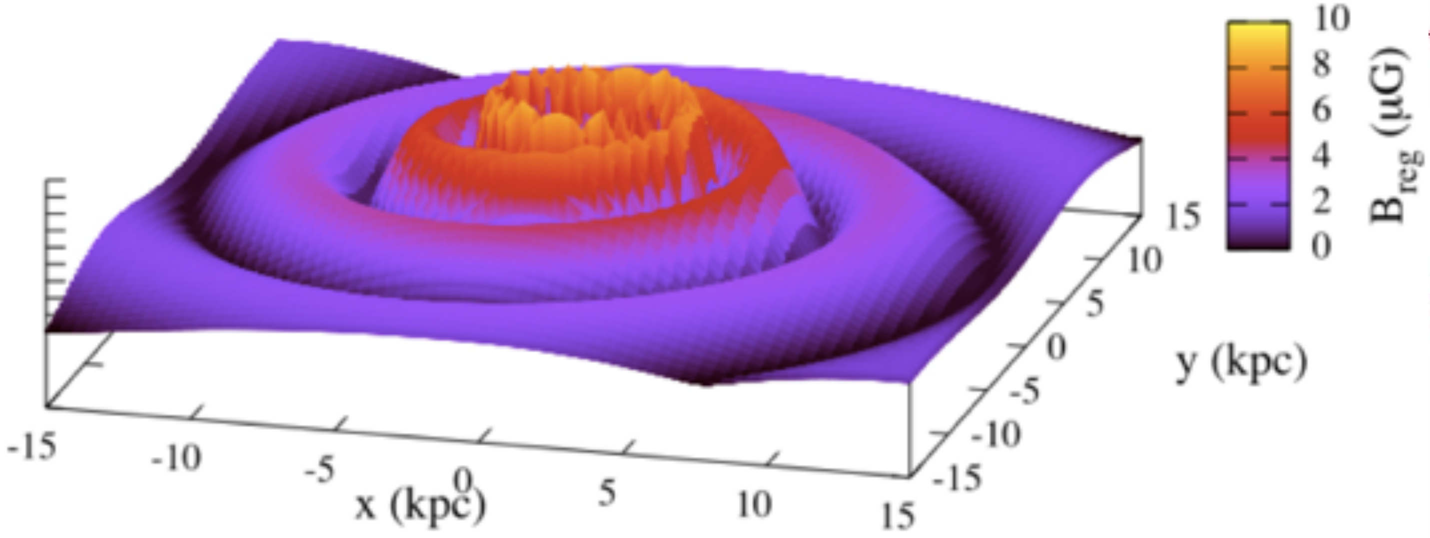

[Jansson & Farrar 2012]

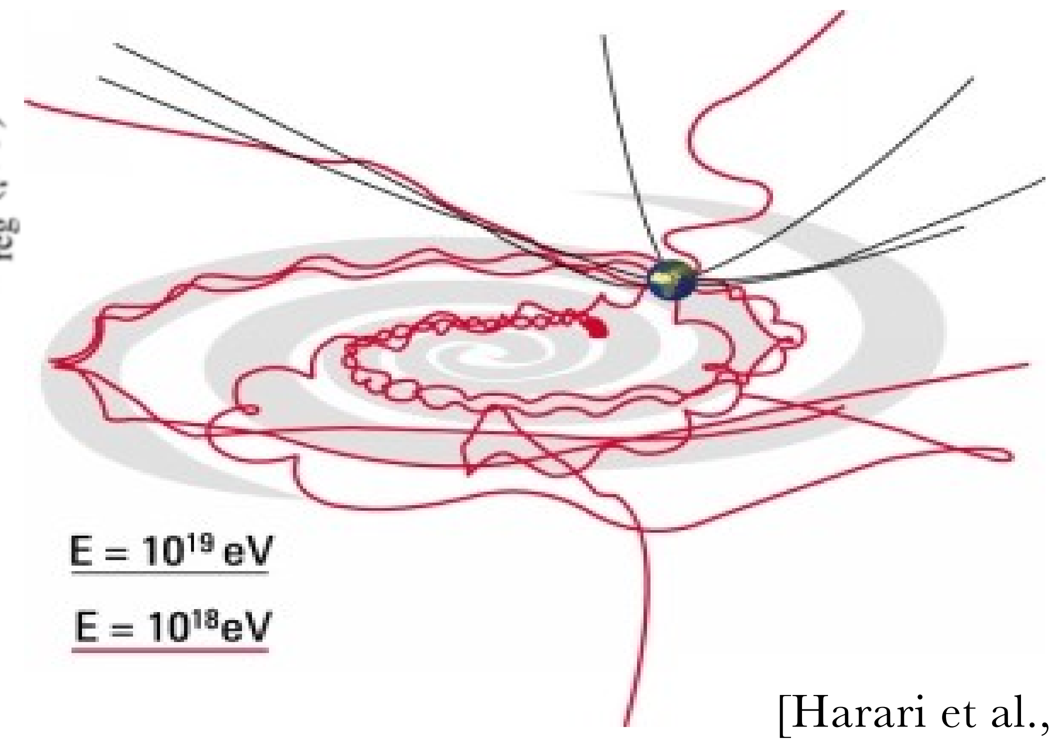

[Harari et al., 1999]

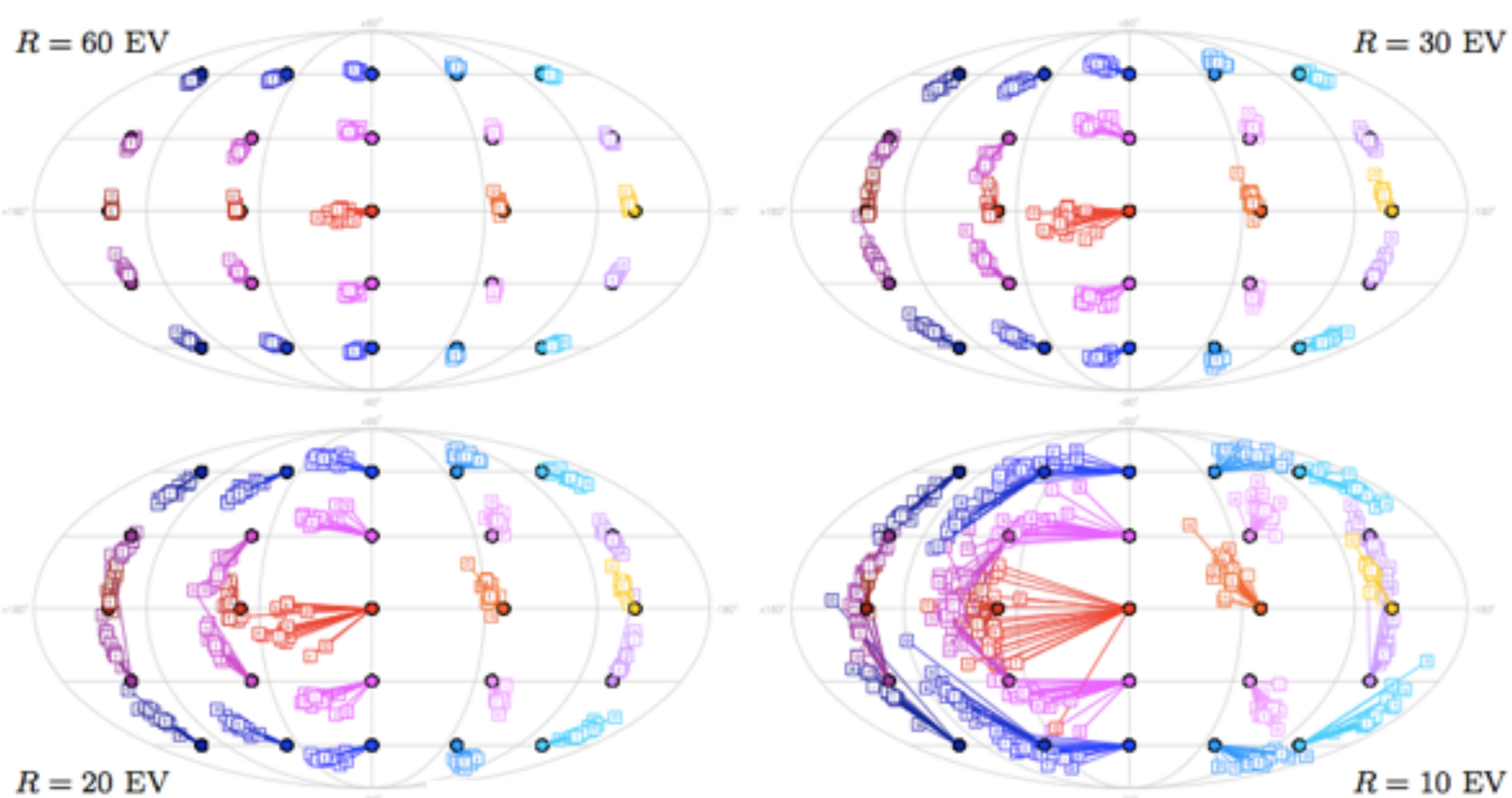

[Unger & Farrar 2017]

At UHE, CRs may be rigid enough to point back to their sources within a few degrees

+ Reduced horizon

➡ Possibility to identify nearby sources?

ii) Large-scale anisotropies at the Auger Observatory

First harmonic in right ascension

- Control of the event rate/directional exposure in right ascension

➡ Fourier expansion of the intensity

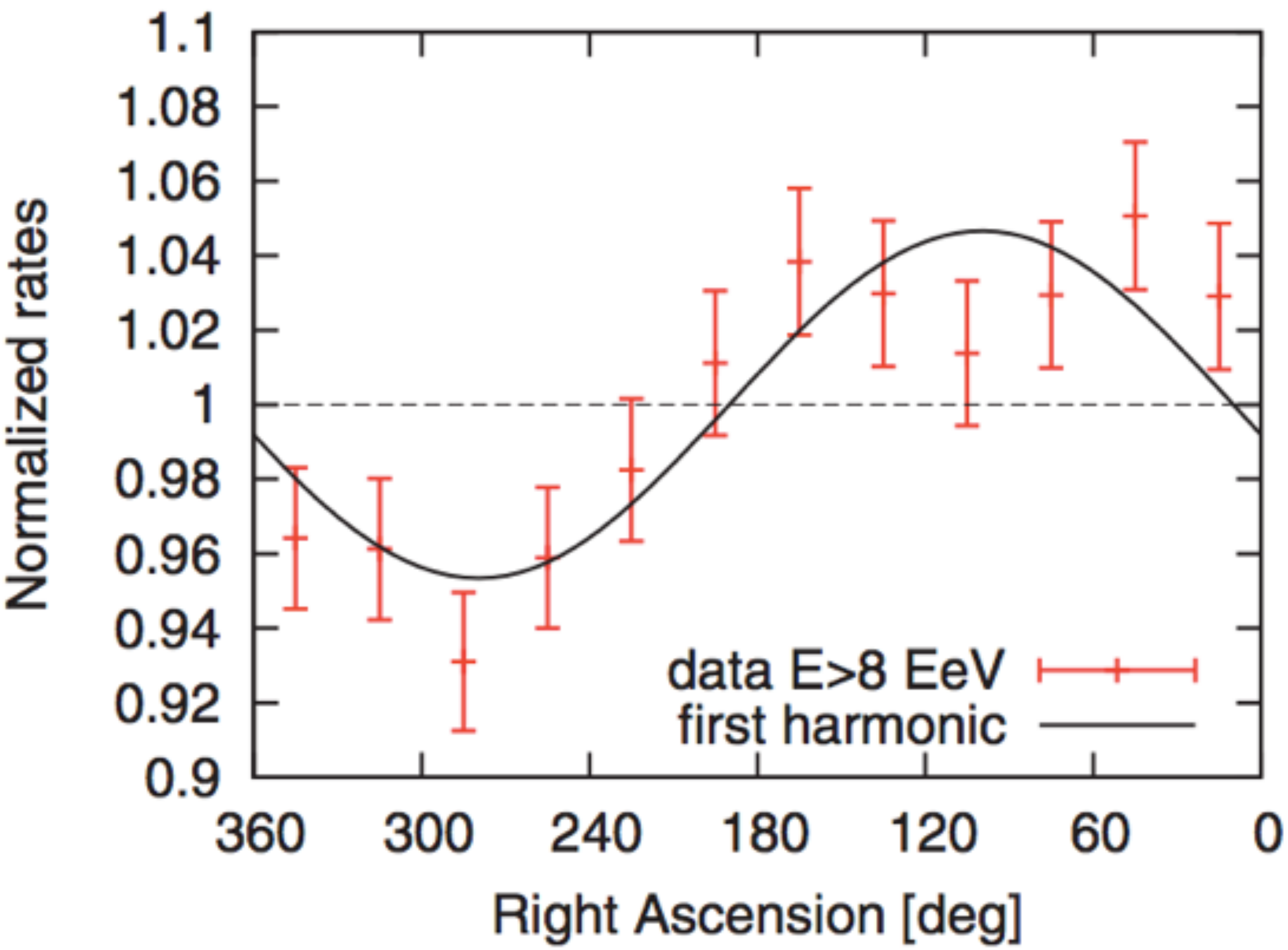

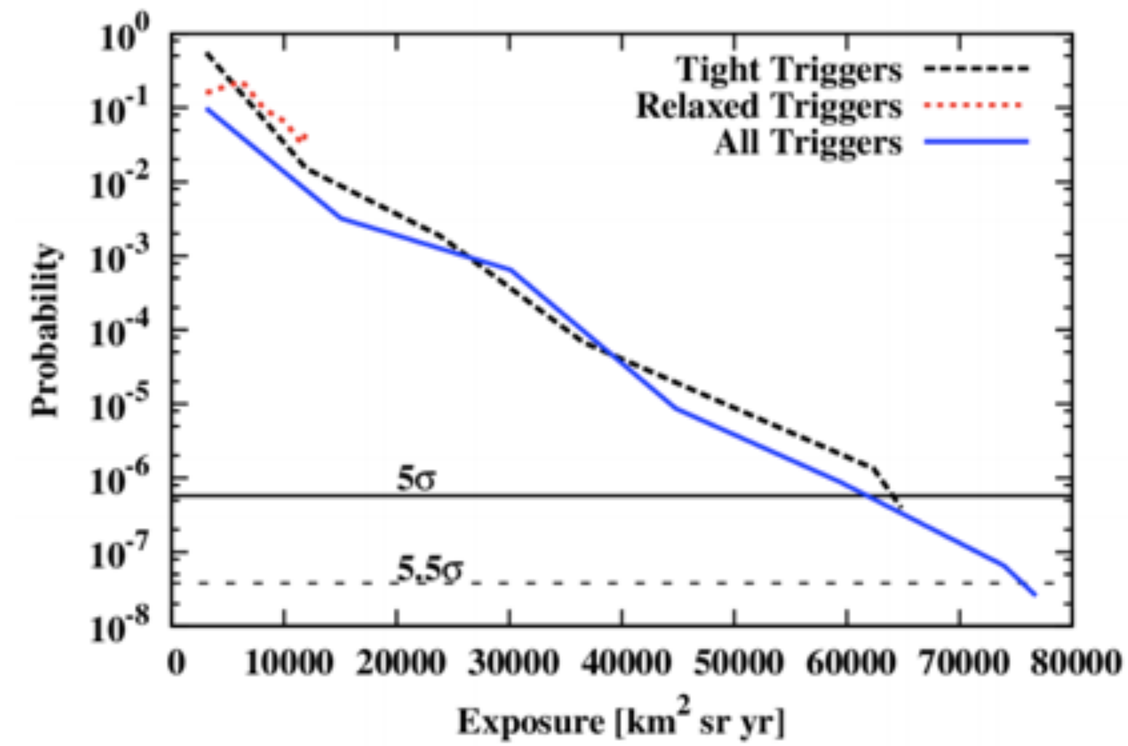

- Detection at >5σ (accounting for the null results in other energy ranges)

Interpretation in terms of a dipole

- Additional first harmonic analysis in local azimuth sensitive to the dipole component along the Earth axis

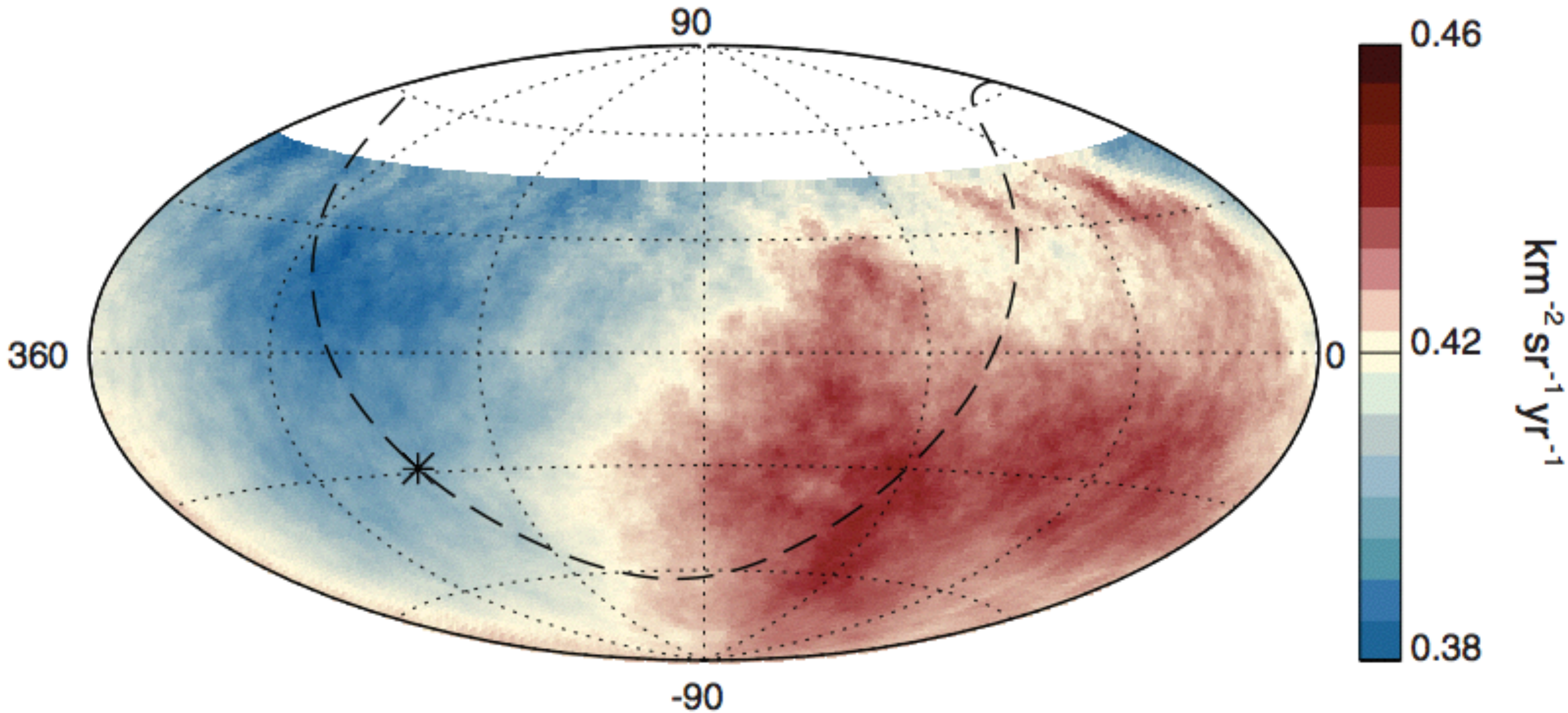

Galactic origin?

- Direction of the dipolar component of the intensity for a Galactic origin

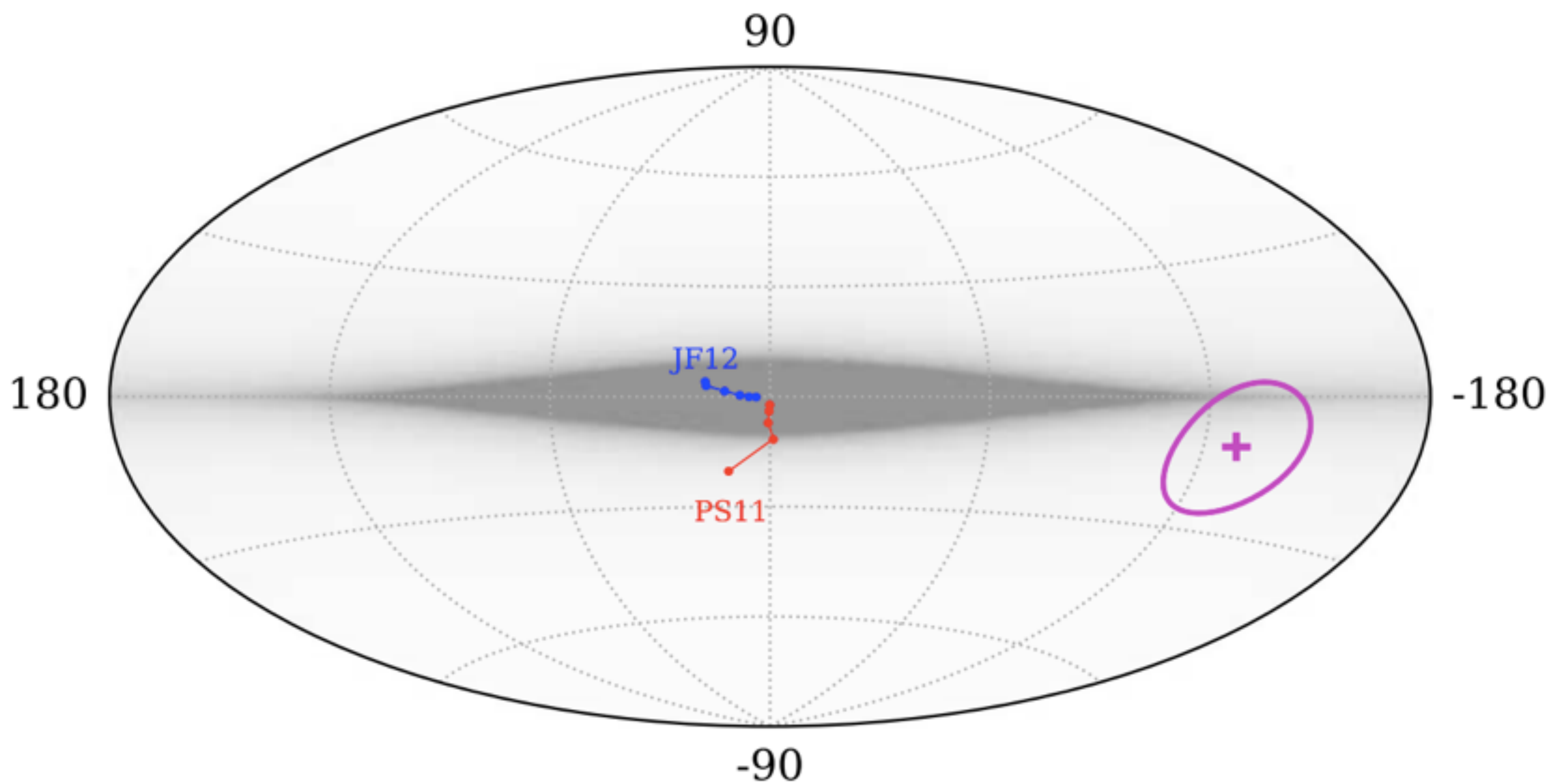

Extragalactic origin

- Dipole component of the 2MRS catalog folded into the GMF

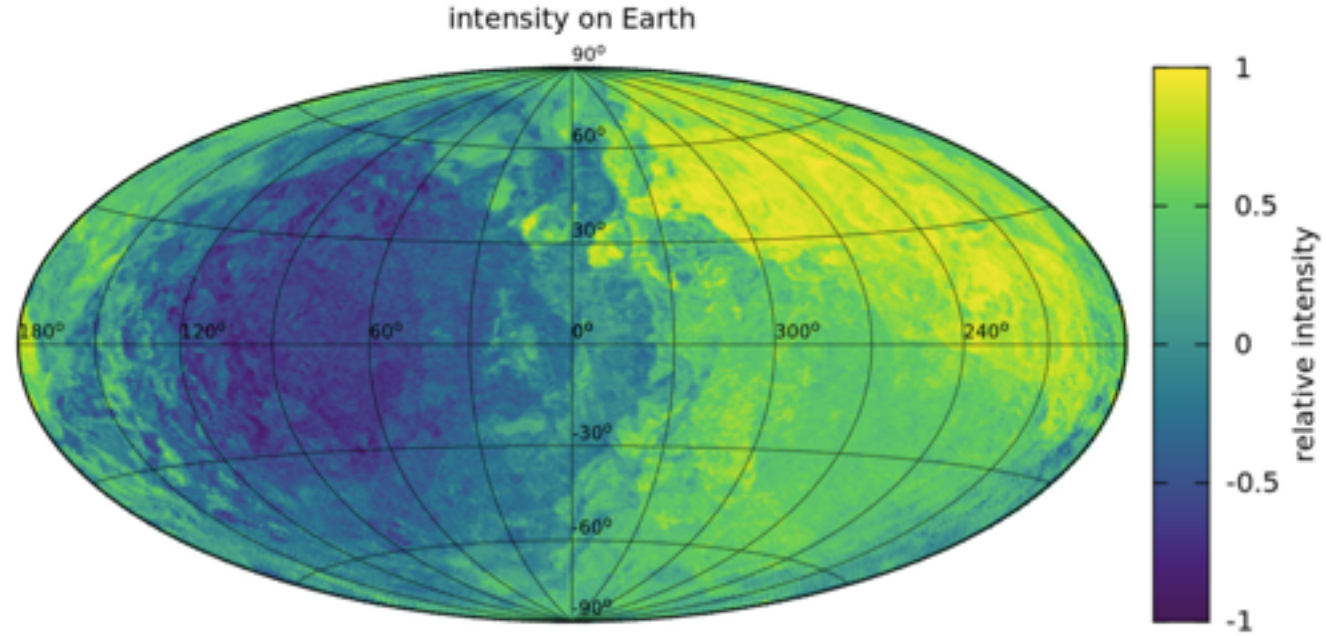

➡ Dipole at the entrance of the Galaxy not 'destroyed' by the GMF (JF12 model here)

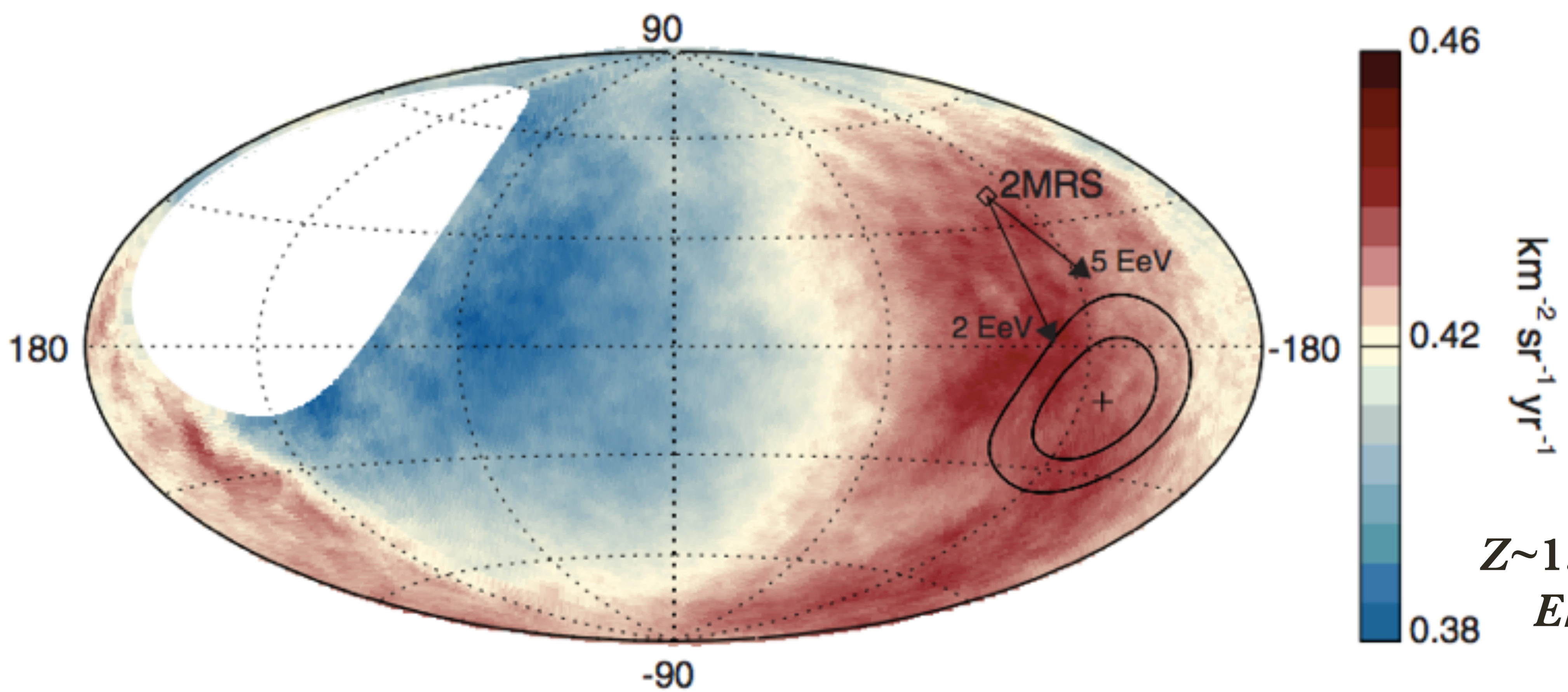

***Z*~1.7-5 at 10 EeV**
***E*/*Z*~2-5 EeV**

Higher-order multipoles?

- Dipole moment following from extragalactic matter
- Higher order multipole signatures to constrain further models?

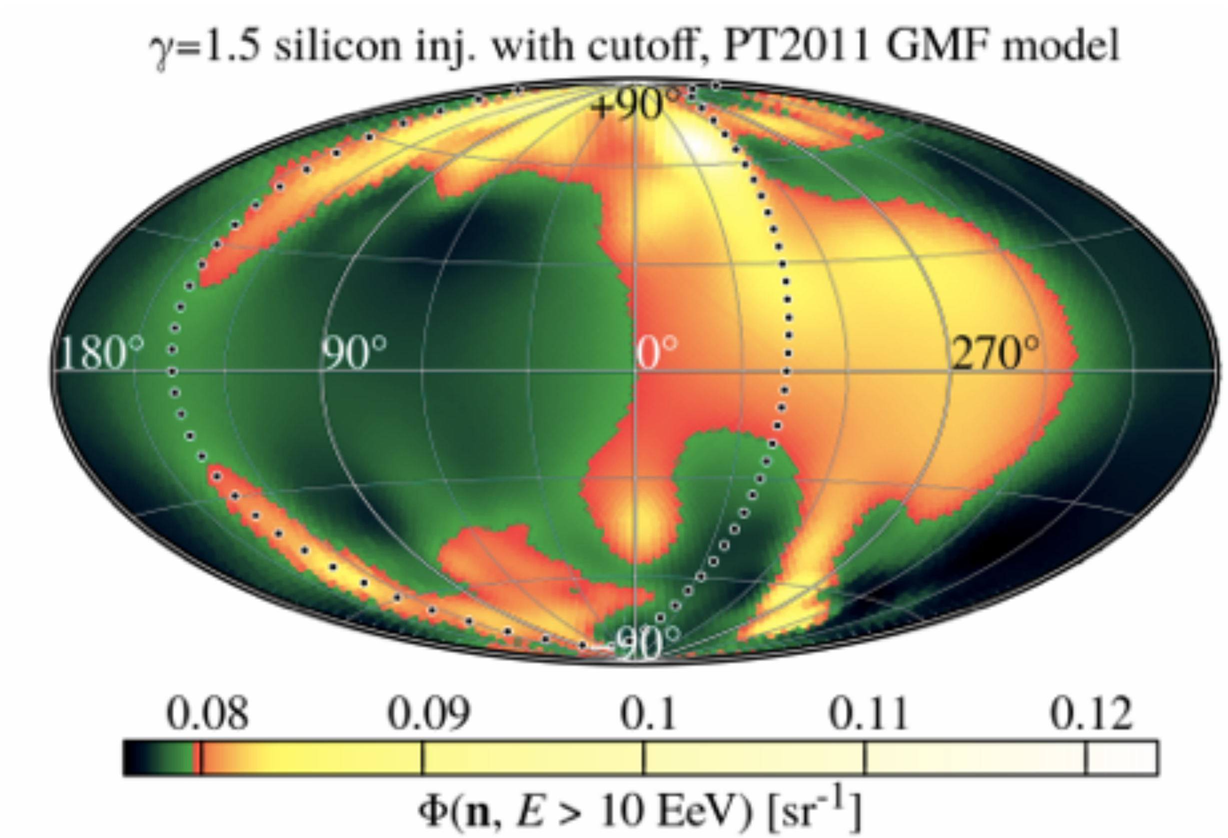

[Di Matteo & Tinyakov, arXiv:1706.02534]

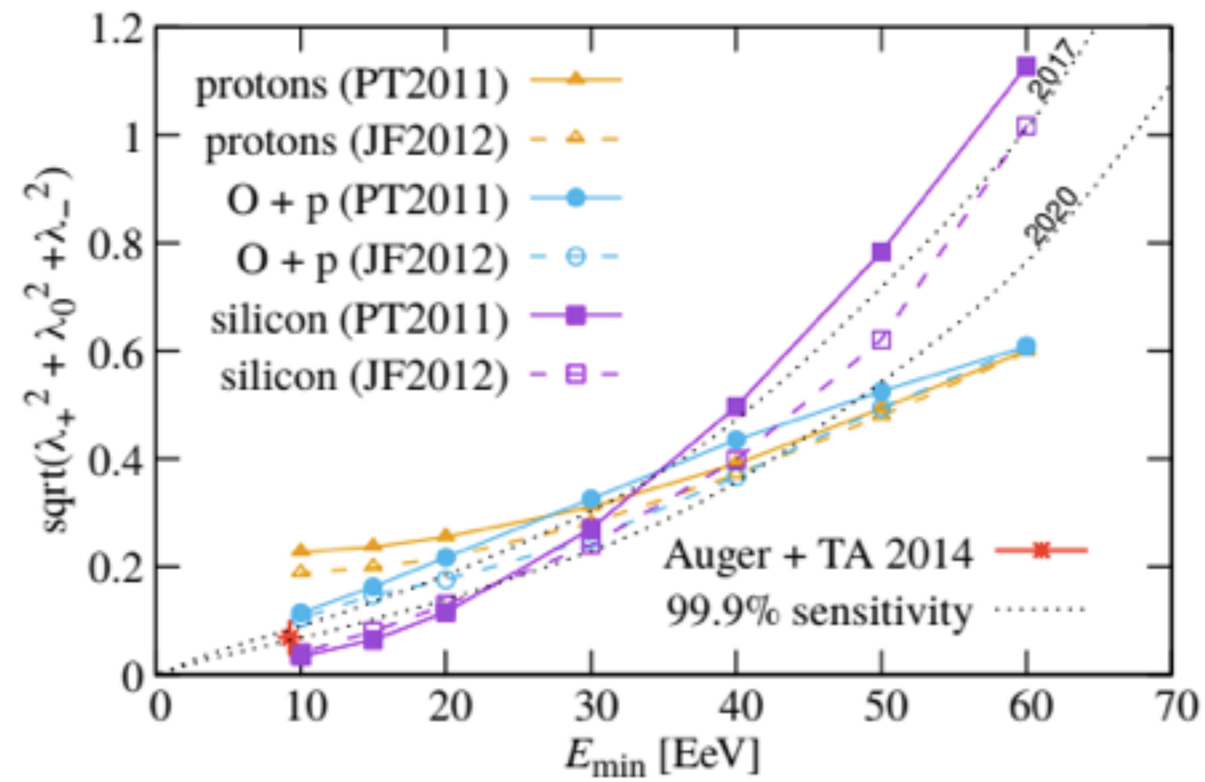

➡ Measurement of high-order multipoles/angular power spectrum?

iii) Multipole analysis with partial-sky coverage

Beyond the dipole moment?

- Multipolar moment as seen through the coverage:

$$b_{\ell m} = \int_{\Delta\Omega} \mathrm{d}\Omega_{\mathbf{n}}\, \tilde{\omega}(\mathbf{n},\Delta E)\Phi(\mathbf{n})\, Y_{\ell m}(\mathbf{n})$$
$$= \sum_{\ell' \geq 0} \sum_{m'=-\ell'}^{\ell'} a_{\ell' m'} \int_{\Delta\Omega} \mathrm{d}\Omega_{\mathbf{n}}\, \tilde{\omega}(\mathbf{n},\Delta E)\, Y_{\ell' m'}(\mathbf{n})\, Y_{\ell m}(\mathbf{n}).$$

- Recovering coefficients *if* $\Phi(\mathbf{n})$ bounded to $\ell_{\max}$:

$$\overline{a}_{\ell m} = \sum_{\ell'=0}^{\ell_{\max}} \sum_{m'=-\ell'}^{\ell'} [K^{-1}_{\ell_{\max}}]^{\ell' m'}_{\ell m}\, \overline{b}_{\ell' m'}.$$

▸ *BUT* exponential degradation of the resolution each time the bound is incremented by 1:

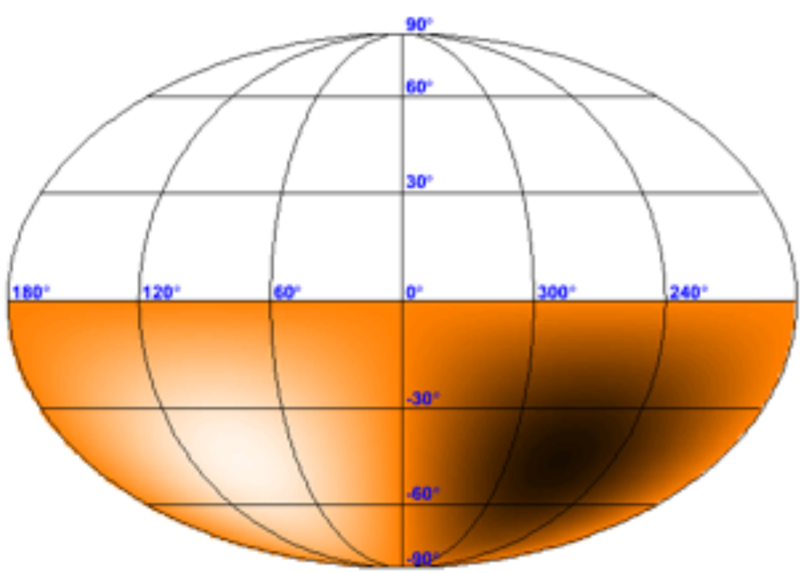

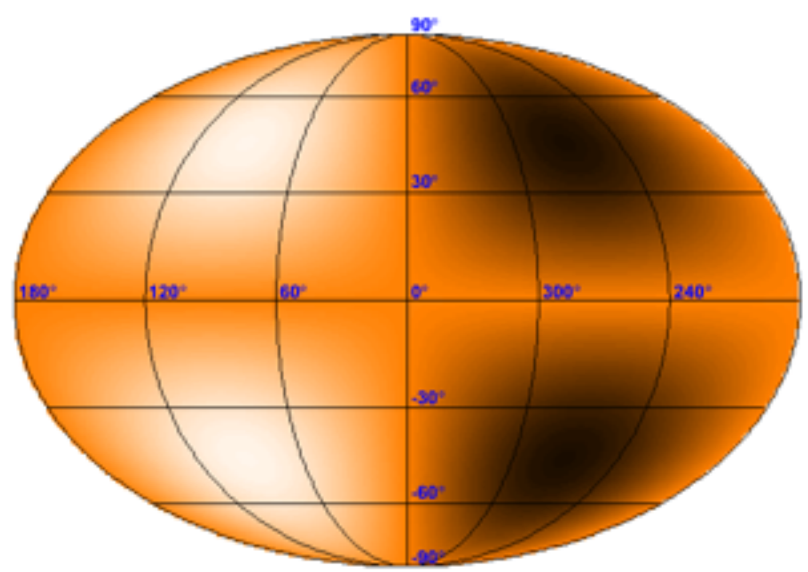

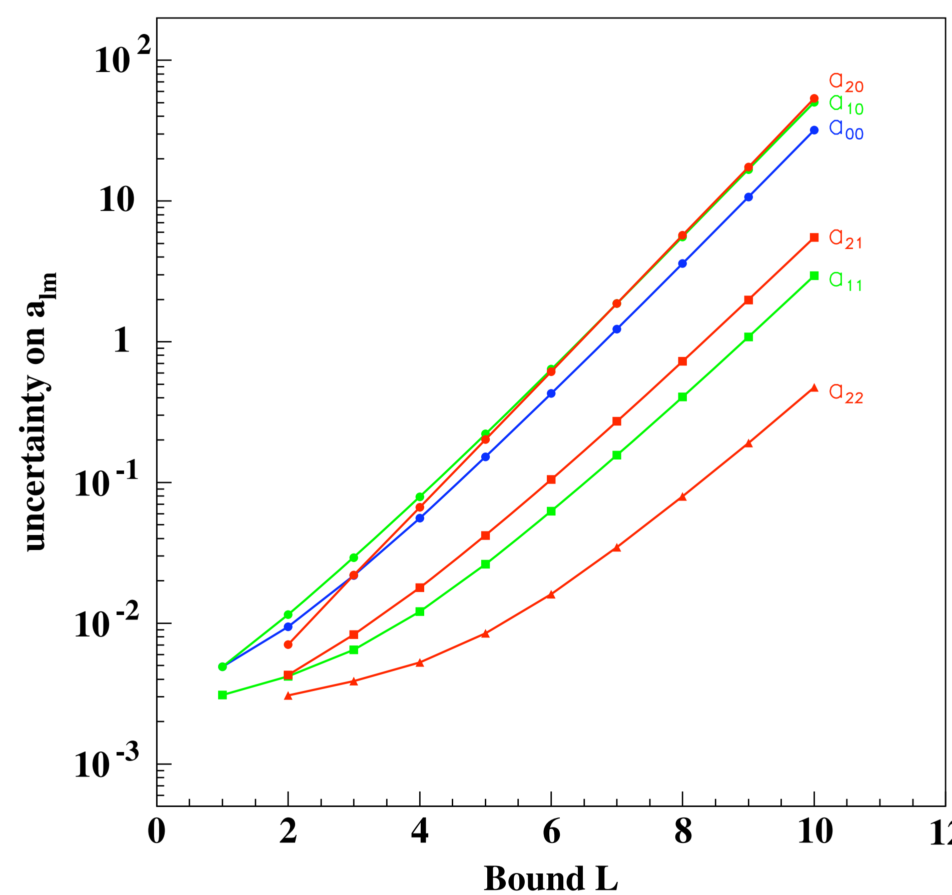

Angular power spectrum—stationarity

$$[K]_{\ell\ell'}^{mm'} = \int_{4\pi} \mathrm{d}\Omega\, Y_\ell^m(\Omega)\omega(\Omega)Y_{\ell'}^{m'}(\Omega).$$

→ mixing matrix for the multipolar moments

$$[M]_{\ell\ell'} = \frac{2\ell'+1}{2}\int_{-1}^{1} \mathrm{d}(\cos\theta)P_\ell(\cos\theta)P_{\ell'}(\cos\theta)\mathcal{W}(\theta).$$

→ mixing matrix for the power spectrum

2pt function of the coverage:

$$\mathcal{W}(\theta) = \int\int \frac{\mathrm{d}\Omega_1\mathrm{d}\Omega_2}{8\pi^2}W(\Omega_1)W(\Omega_2)\delta(\cos\theta - \cos\theta_{12}).$$

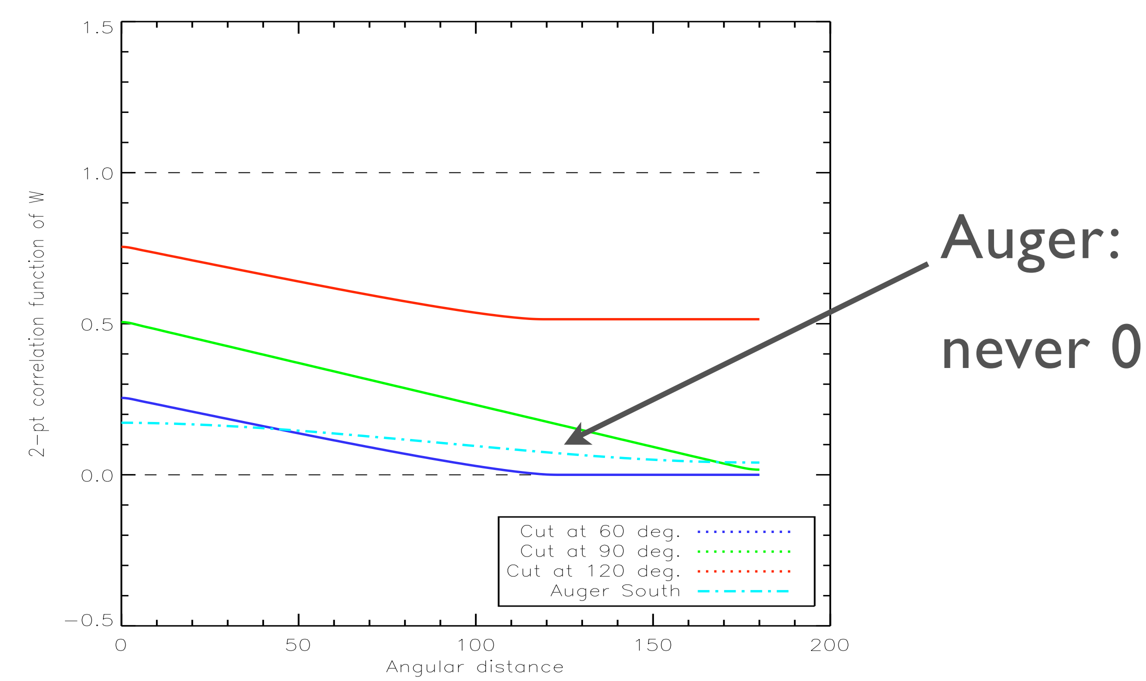

➡ if **<ϕ(n)>=0** and **<ϕ(n)ϕ(n')>=ξ(n.n'),** then it can be shown that

$$\langle C_\ell^{\mathrm{exp}}\rangle = \sum_{\ell'} M_{\ell\ell'}^{-1}\langle\tilde{C}_{\ell'}\rangle = C_\ell + \frac{4\pi}{N}\frac{f_1^2}{f_2}.$$

«Poisson» noise term

estimated as in the case of full-sky coverage

«true» power spectrum

Hypothesis: Stationarity

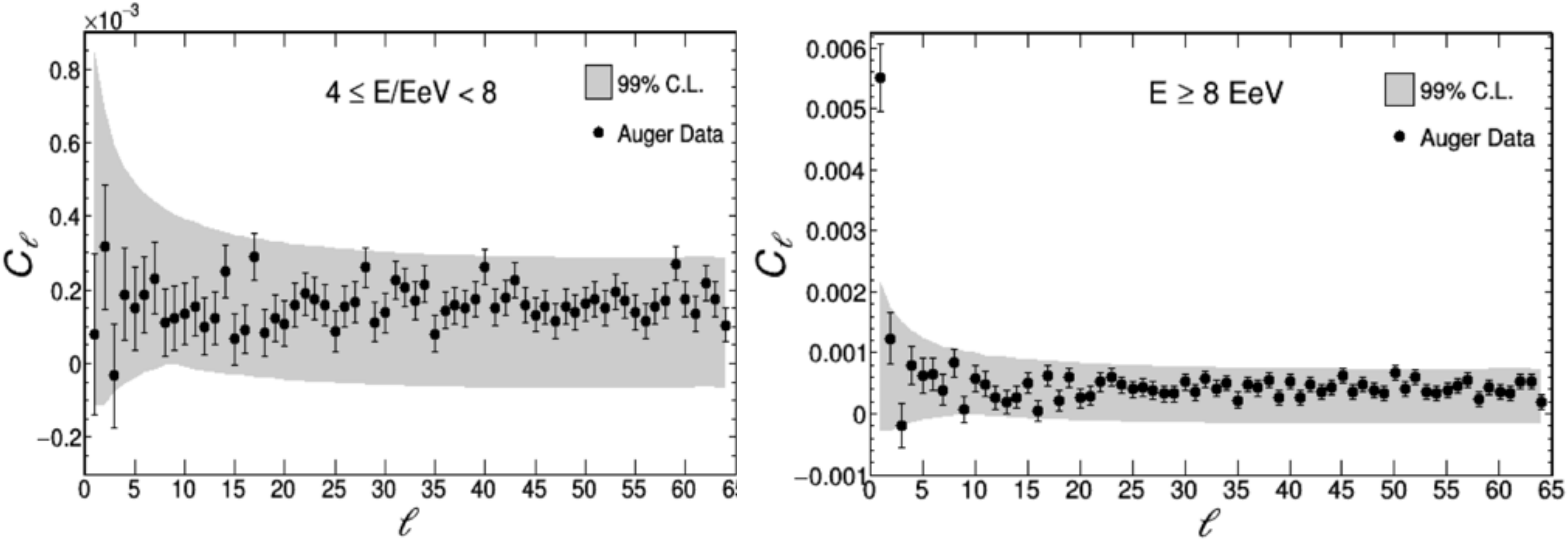

Under stationarity assumptions, no signal beyond the dipole moment

iv) Multipole analysis with full-sky coverage

(Last update: ICRC 2015)

Meta-analysis of Auger and TA data

Auger+TA: full-sky coverage with full efficiency >10 EeV, *but*…

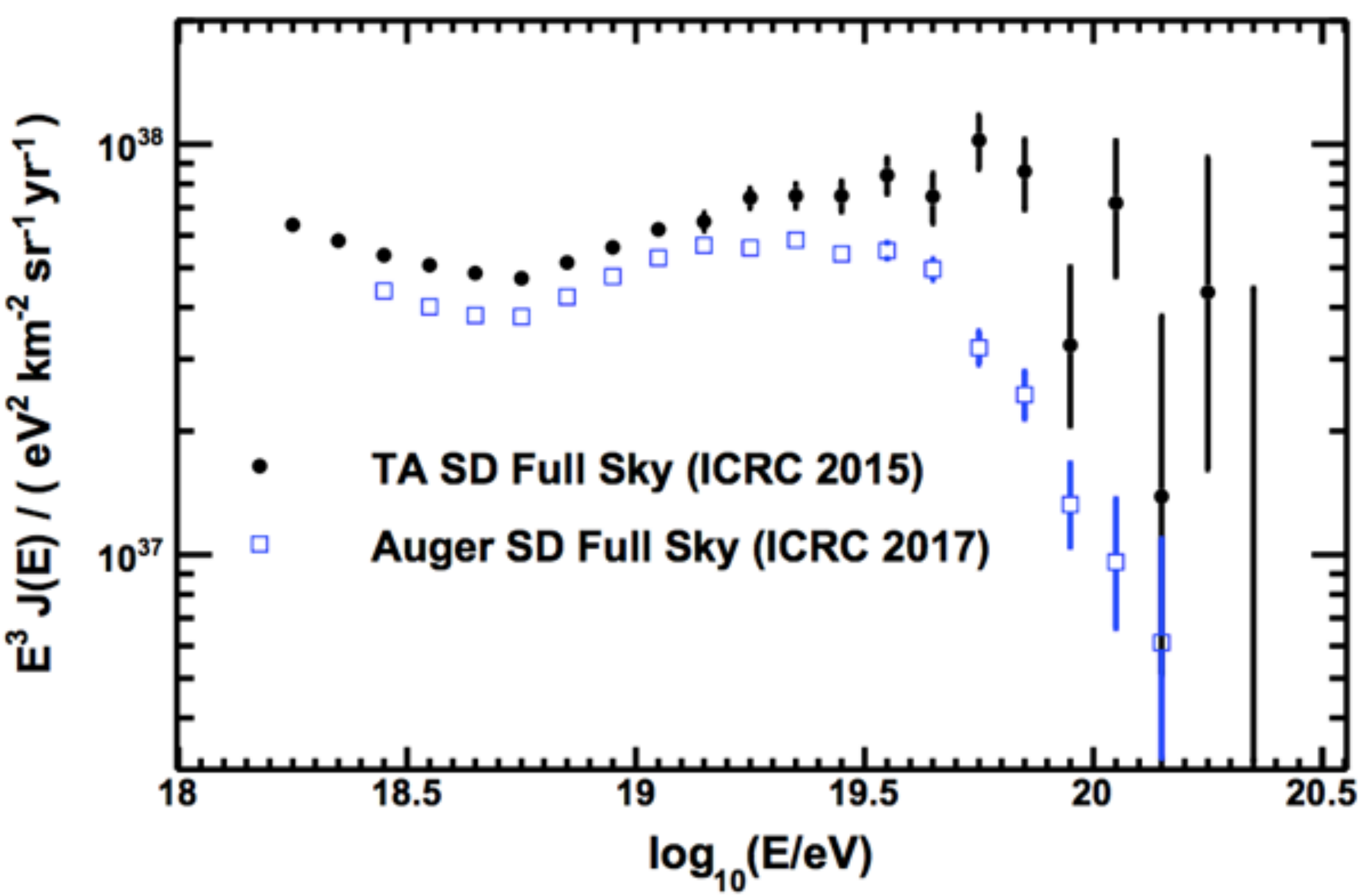

Uncertainty on energy scale

Auger: 14%

TA: 21%

Intensity in the common band

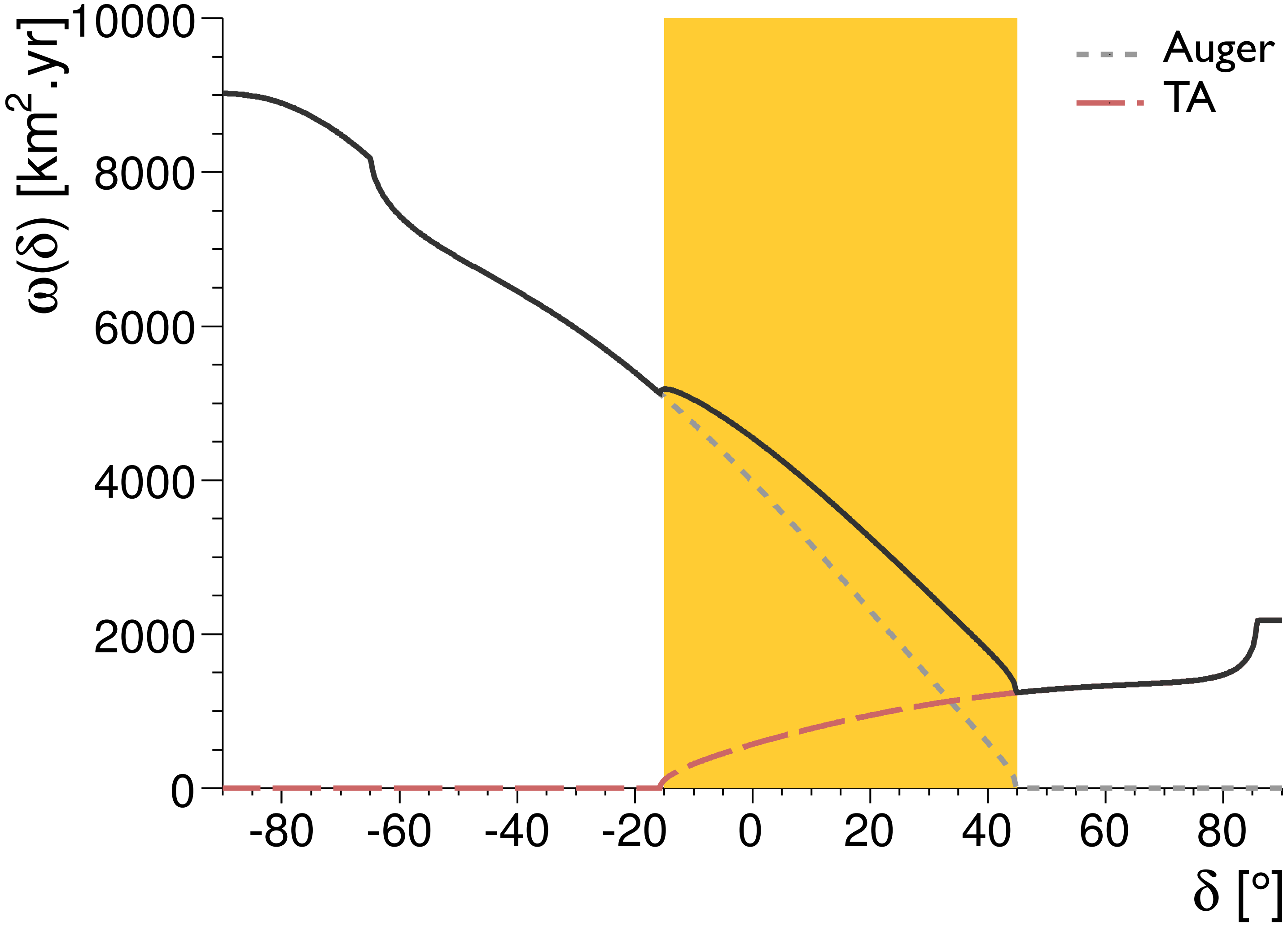

- Aim: guarantee the same intensity in the common field of view

- If anisotropies, possible distortions by the directional exposure functions

➡ Remove distortions induced from different directional exposures in case of anisotropies:

$$J_{1/\omega}(E) = \frac{1}{\Delta\Omega\Delta E}\sum_{i=1}^{N}\frac{1}{\omega(\delta_i)}$$

➡ Tune the energy scale to get $\mathcal{J}_{\mathrm{Auger}}(>E)=\mathcal{J}_{\mathrm{TA}}(>E)$ in the common f.o.v.

Performances

$$\sigma_{\ell m}^2 \simeq \frac{4\pi f_1 N}{\Omega_0^2}\int d\mathbf{n}\left\langle \frac{\mu_r(\mathbf{n})}{\bar{\mu}_r^2(\mathbf{n})}\right\rangle_P Y_{\ell m}^2(\mathbf{n}) + \frac{N^2}{\Omega_0^2}\int d\mathbf{n}d\mathbf{n}'\left[\left\langle \frac{\mu_r(\mathbf{n})\mu_r(\mathbf{n}')}{\bar{\mu}_r(\mathbf{n})\bar{\mu}_r(\mathbf{n}')}\right\rangle_P - 1\right] Y_{\ell m}(\mathbf{n})Y_{\ell m}(\mathbf{n}').$$

Poisson — Combination of experiments

Degradation of resolution w.r.t. a perfect detector with full-sky coverage

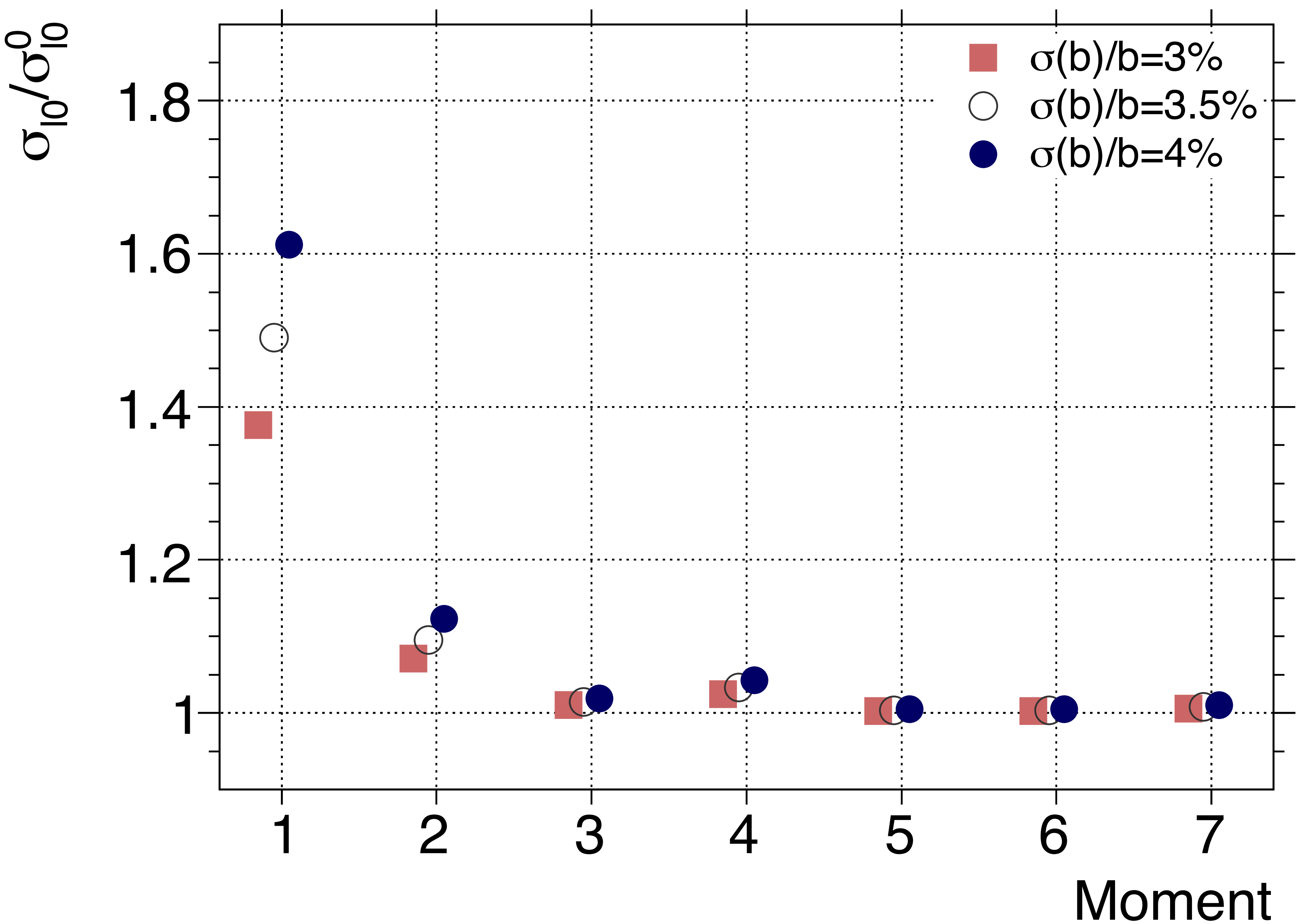

Full-sky map

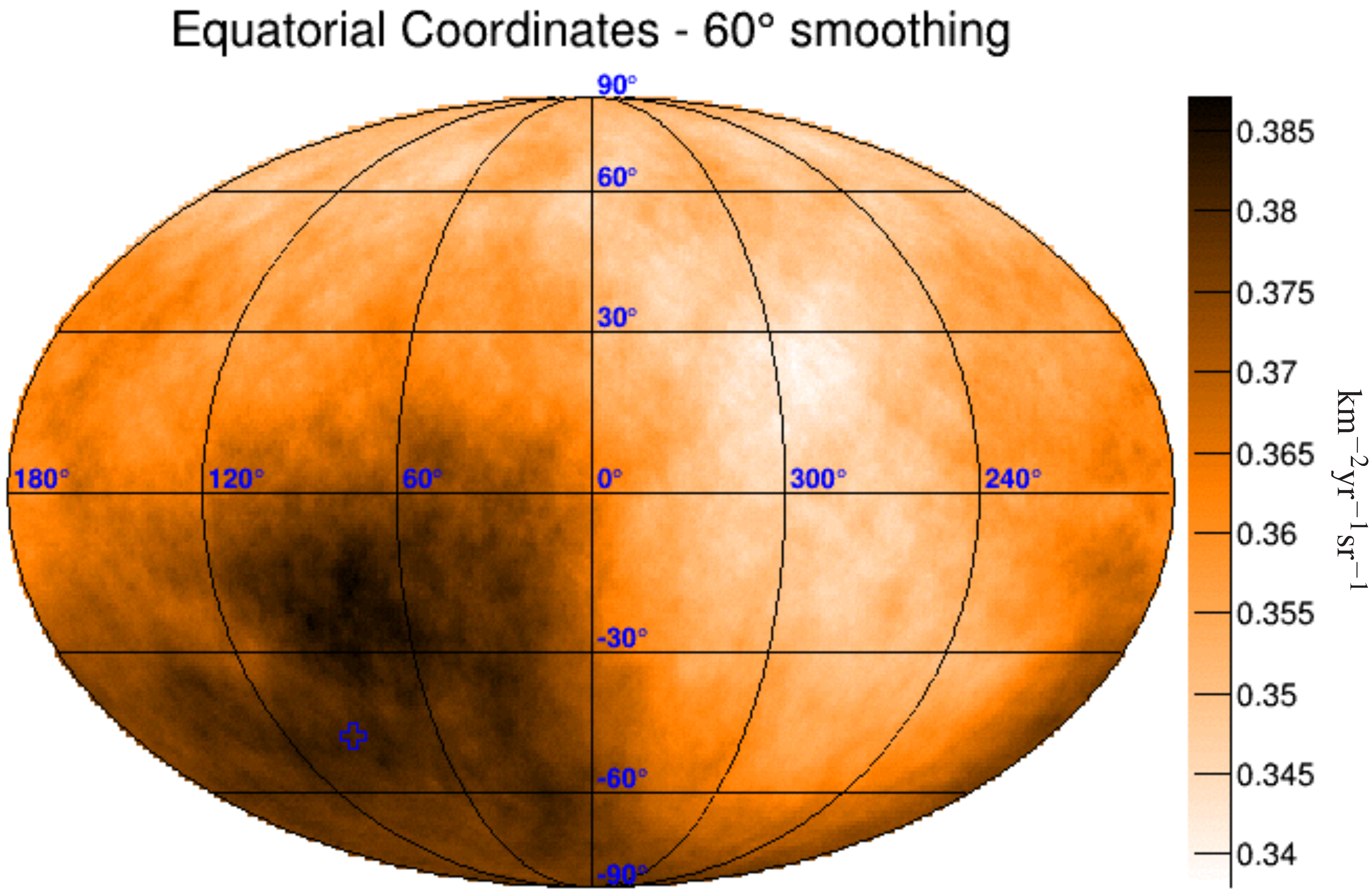
Equatorial Coordinates - 60° smoothing
90°
60°
30°
180°
120°
60°
0°
300°
240°
-30°
-60°
-90°
0.385
0.38
0.375
0.37
0.365
0.36
0.355
0.35
0.345
0.34
km^{-2}yr^{-1}sr^{-1}

Dipole/Quadrupole moments

$$\Phi(\mathbf{n}) = \frac{\Phi_0}{4\pi}\left(1 + r\,\mathbf{d}\cdot\mathbf{n} + \lambda_+(\mathbf{q}_+\cdot\mathbf{n})^2 + \lambda_0(\mathbf{q}_0\cdot\mathbf{n})^2 + \lambda_-(\mathbf{q}_-\cdot\mathbf{n})^2 + \cdots\right)$$

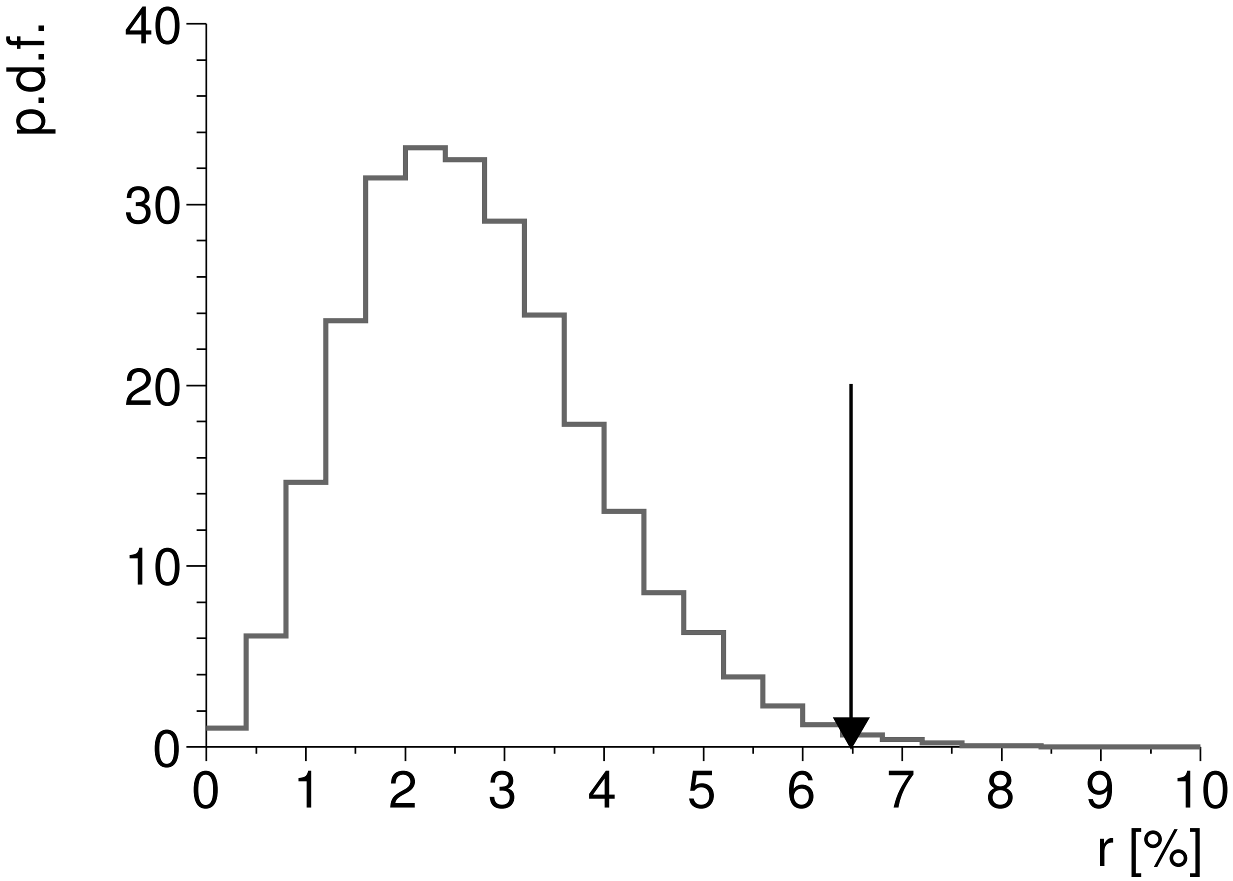

Dipole amplitude

$r = (6.5\pm1.5)\%$, $P = 5\ 10^{-3}$

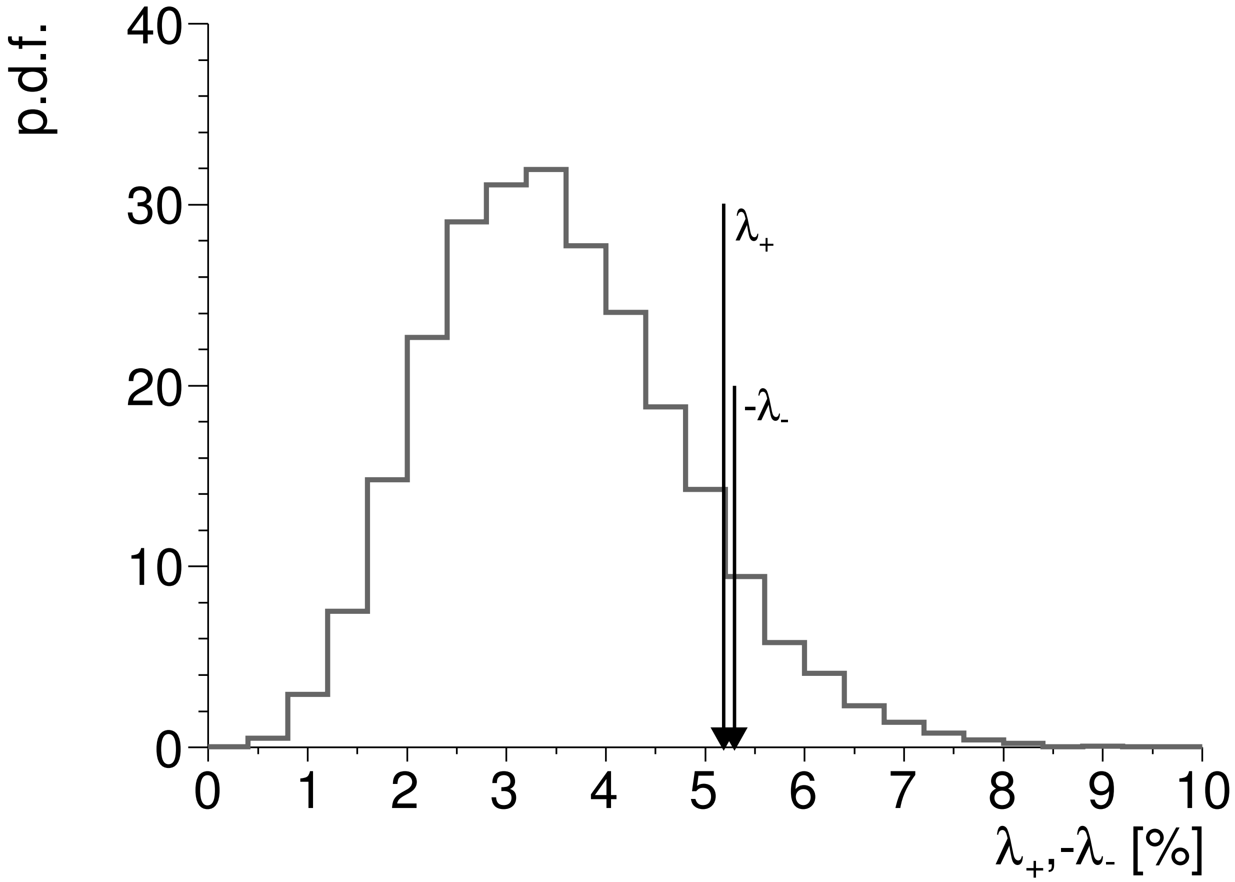

Quadrupole amplitudes within fluctuations

Angular power spectrum

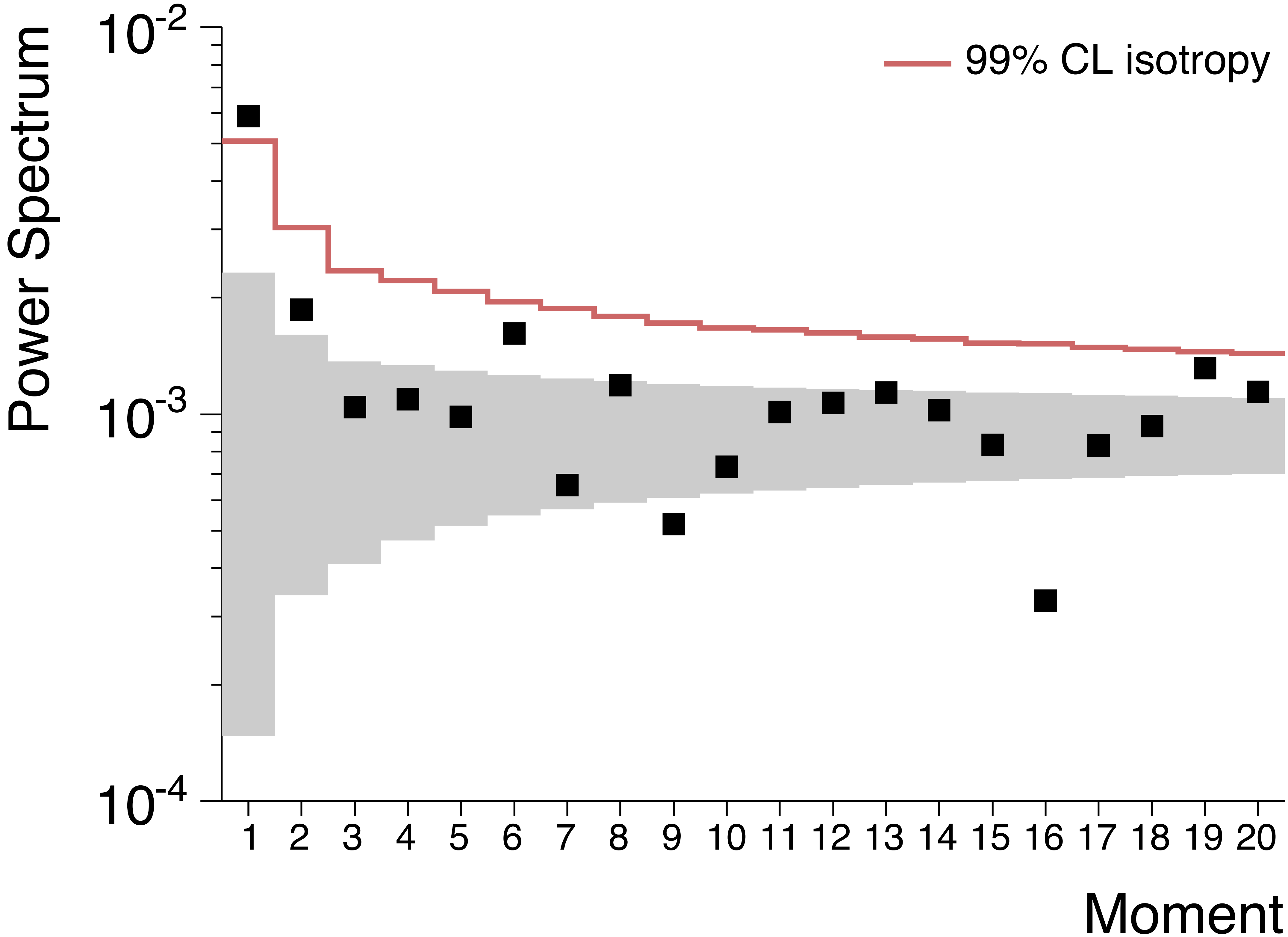

v) The highest energies

Searches for hot spots

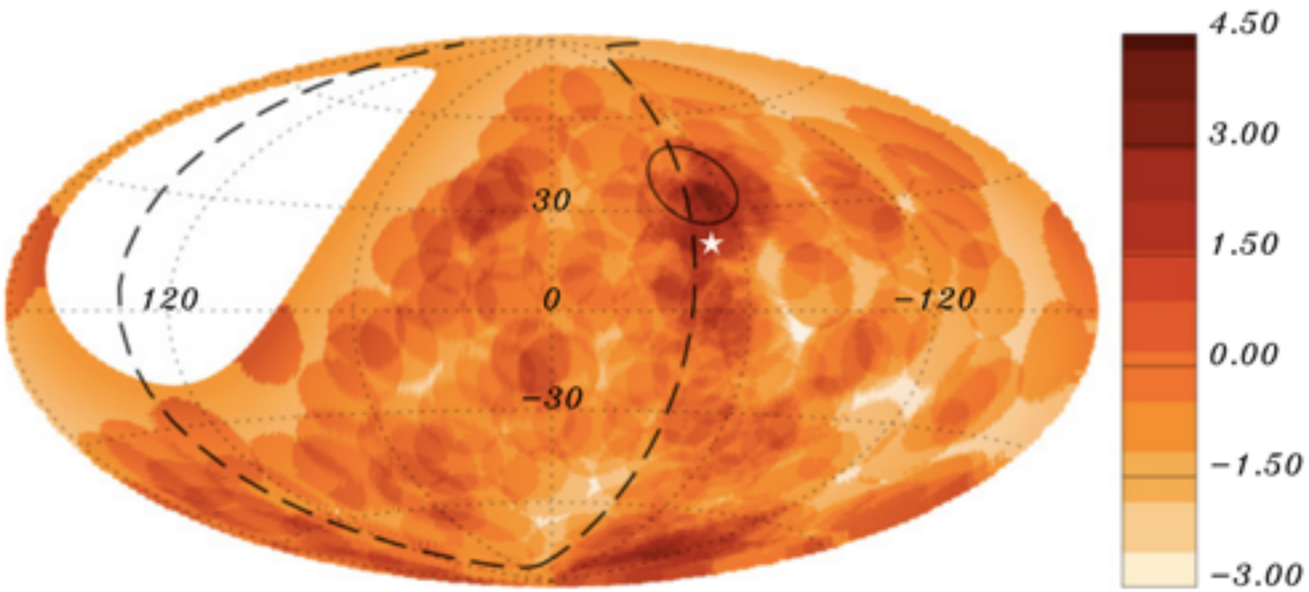

- Scan on energy threshold E and circular window radius Ψ to compute the obs/exp number of events
- 4.3 σ for E>54 EeV and Ψ=12°
- Post-trial p-value: 69%

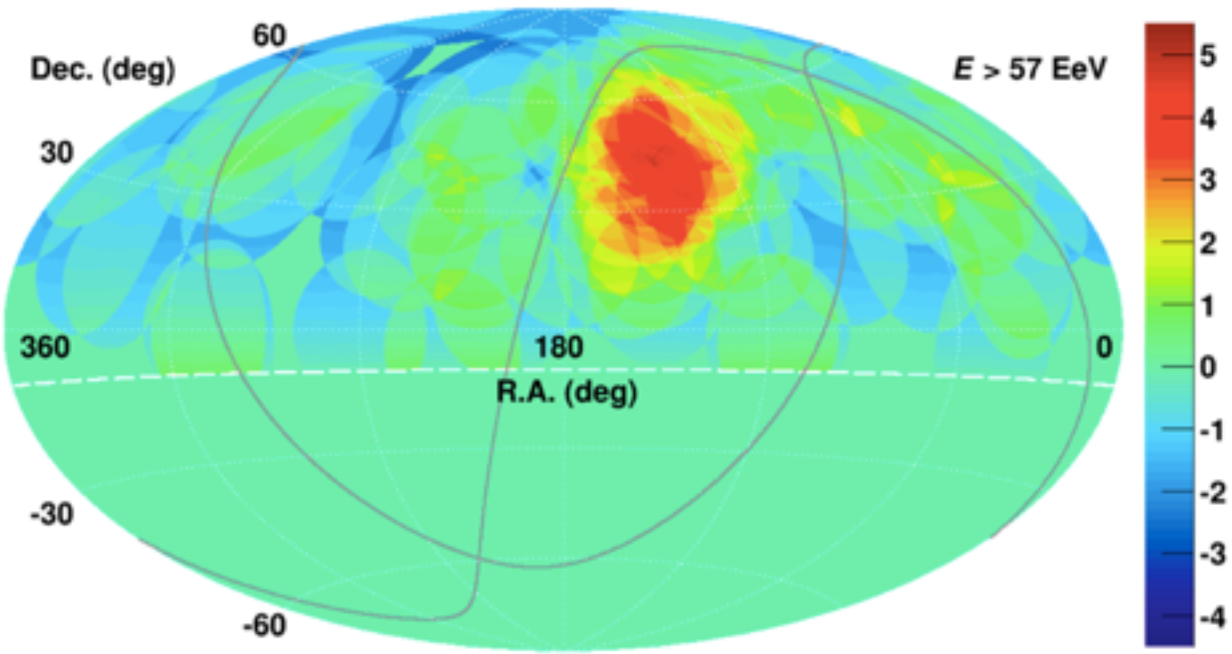

- 134 events >57 EeV, 34 within the 25° window (13.5 exp.)
- Post-trial significance: P~1.0 10^{-3} (3.0σ)

Selection of *non-thermal* sources

Selected from the 2FHL catalog (*Fermi*-LAT, >50 GeV), within 250 Mpc
[Ackermann *et al.*, 2016]
(leptonic processes preferred)

Selected from *Fermi*-LAT search list (HCN survey) within 250 Mpc, with radio flux>0.3 Jy
[Gao & Salomon, 2005]
(hadronic processes preferred)

Assumption: UHECR flux ∝ non-thermal photon flux

➡ Reasonable for UHECRs and gamma rays originating from the same population of sources producing CRs at a similar rate from low energies to the highest ones, CRs which then undergo energy losses in calorimetric environments

Test statistics of alternative vs null

Luminosity distribution: **non-equal** sources,
flux may be dominated by strong local sources

☞ Analysis method: test arrival directions vs **density maps**

null

$L(-,0) = \Pi_{\text{events}}[\text{exposure}](\mathbf{n}_i)$

alternative

$L(\vartheta,\alpha) = \Pi_{\text{events}}[\text{exposure} \times \text{model}(\vartheta,\alpha)](\mathbf{n}_i)$

α: signal fraction

ϑ: search radius (no magnetic offset)

model: $[\alpha \times \text{sources} + (1-\alpha) \times \text{isotropy}] \otimes \text{Gauss}(\vartheta)$

Test statistics (TS): likelihood ratio

- $TS = 2 \ln(L(\vartheta,\alpha)/L(-,0))$
- **Nested** hypotheses: TS is $\boldsymbol{\chi}^2$-distributed with 2 d.o.f. (2 free parameters ϑ,α)

p-value rejection of the null hyp.

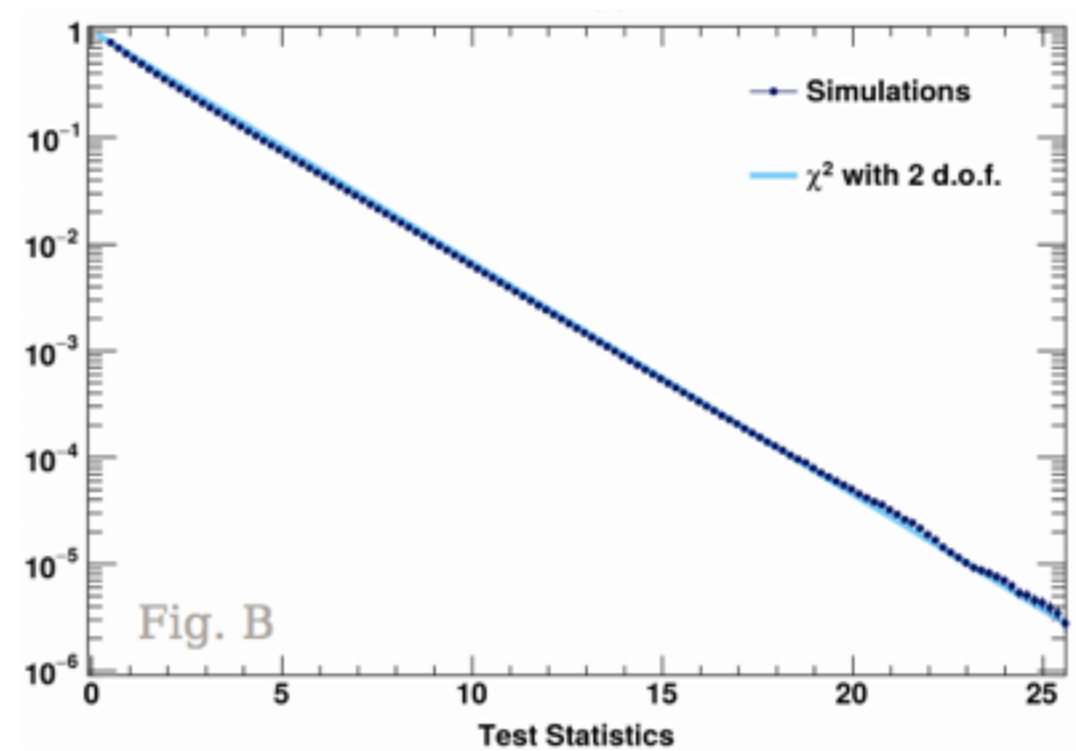

Best fit and residual maps (through Auger f.o.v.)

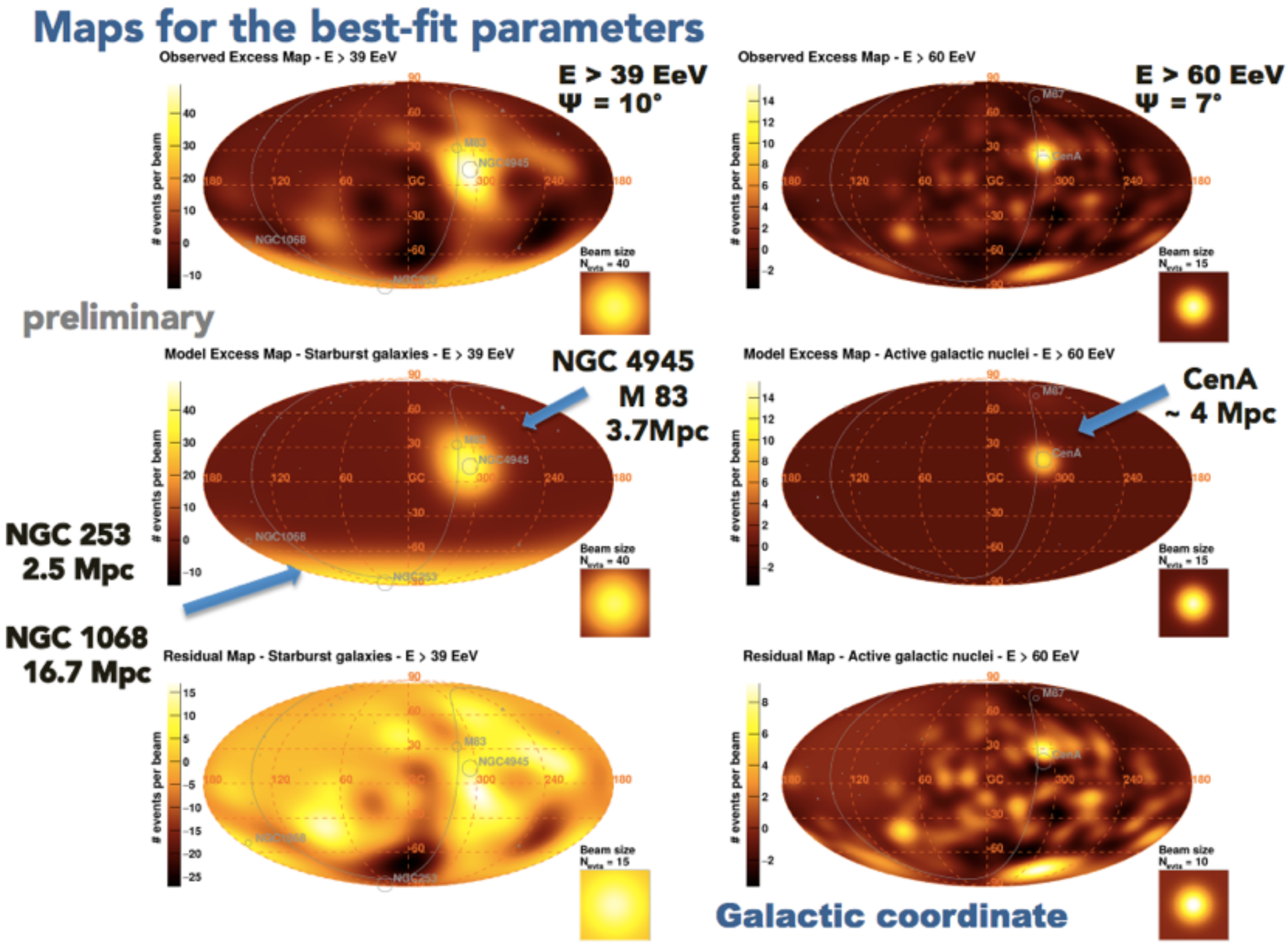

Best fit parameters

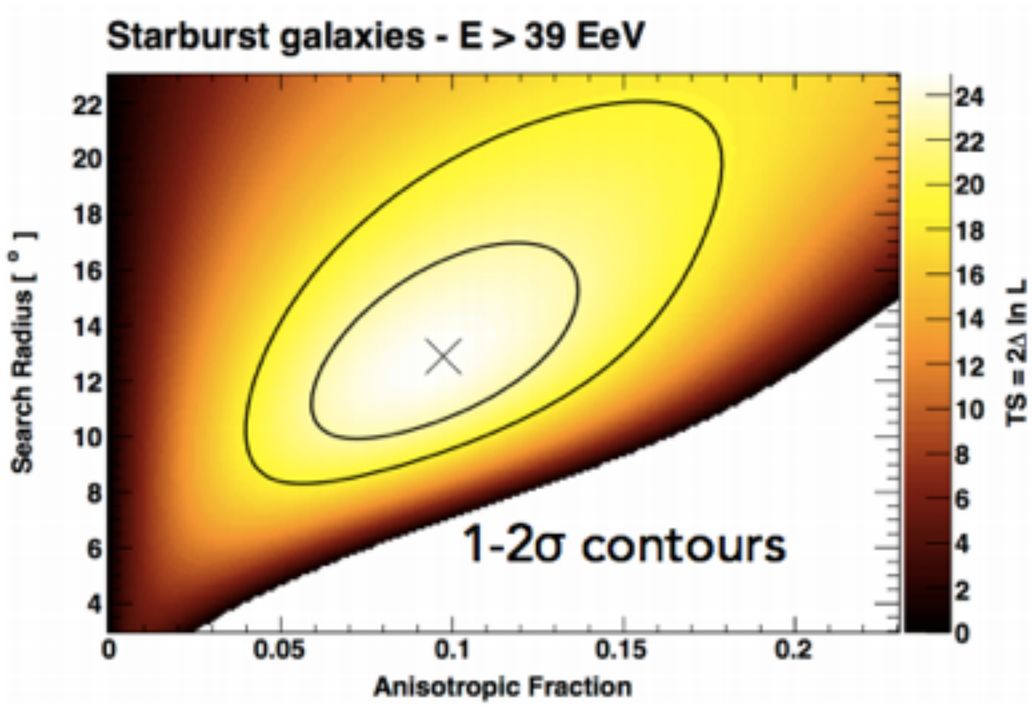

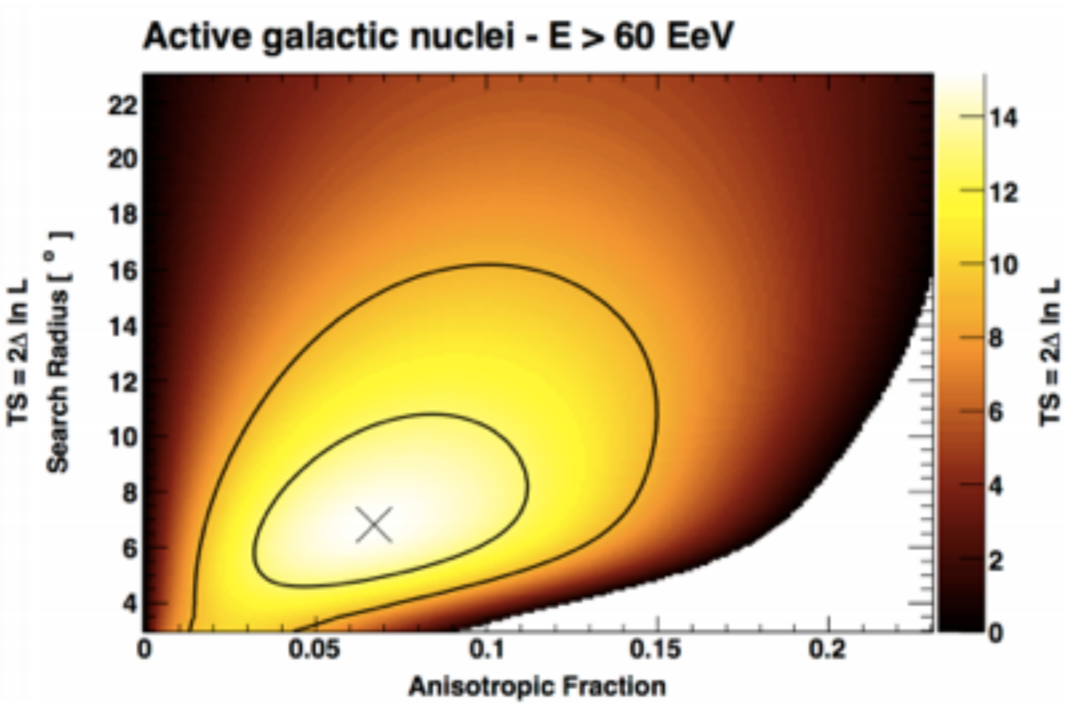

Starburst Galaxies

f_{ani} = 10%, Ψ = 13°

TS = 24.9 ⟶ *p-value* 3.8×10^{-6}

Post-trial probability

3.6×10^{-5} (~4 σ)

γ-ray detected AGNs

f_{ani} = 7%, Ψ = 7°

TS = 15.2 ⟶ *p-value* 5.1×10^{-4}

Post-trial probability

3×10^{-3} (~ 2.7 σ)

- Best indication to reject isotropy provided by the SBG model
- SBG model also preferred to the AGN one in a direct ‘contest’

Auger+TA?

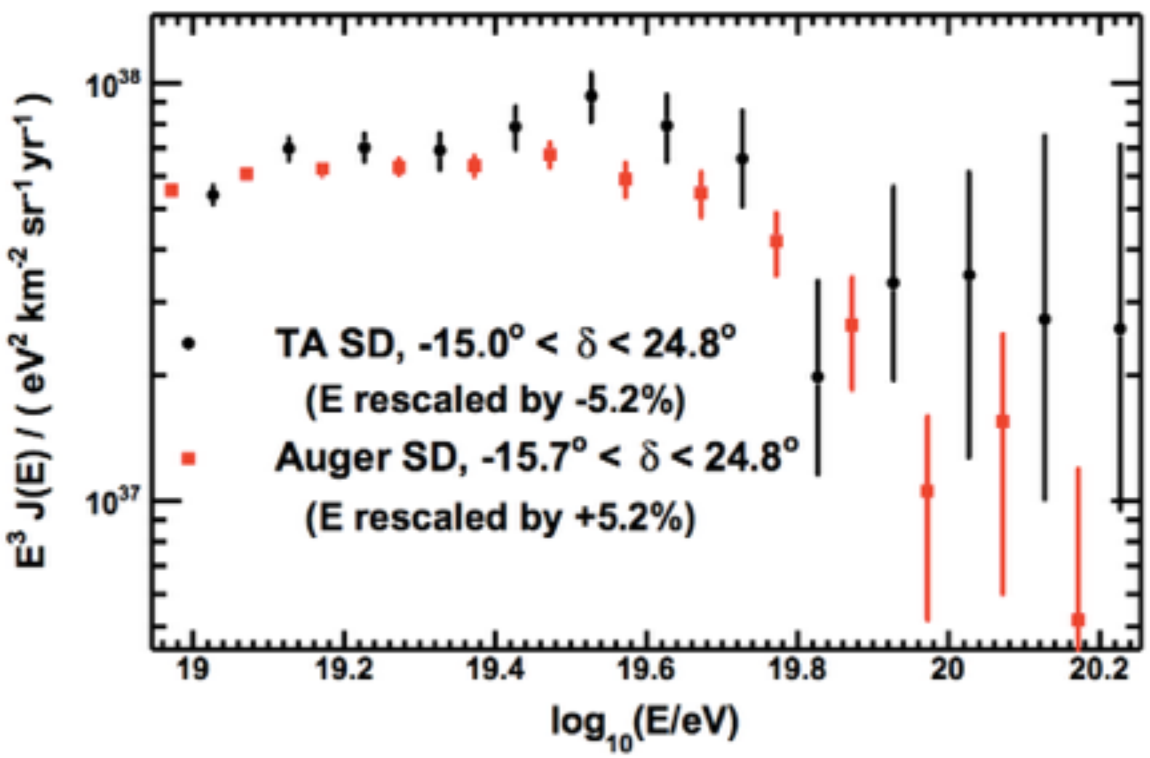

Energy-dependent systematic…

First attempt [UHECR2016]

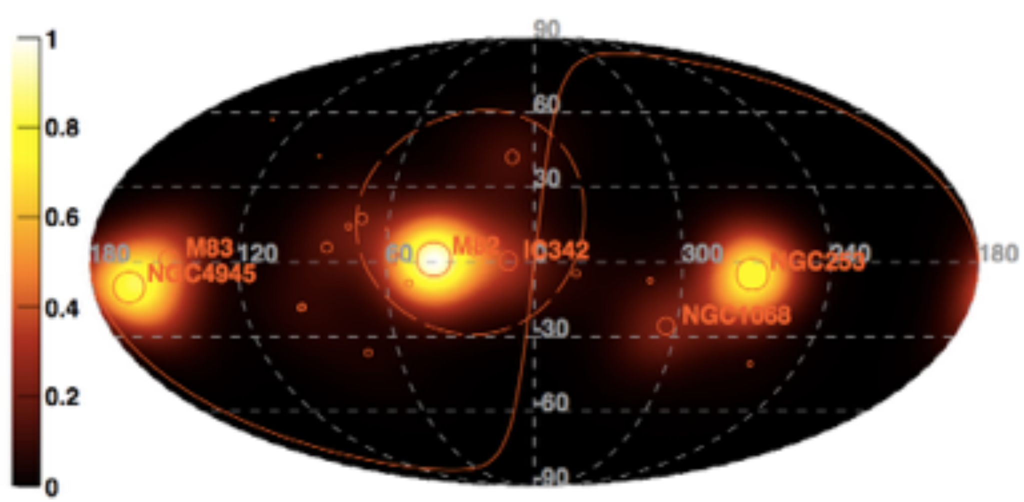

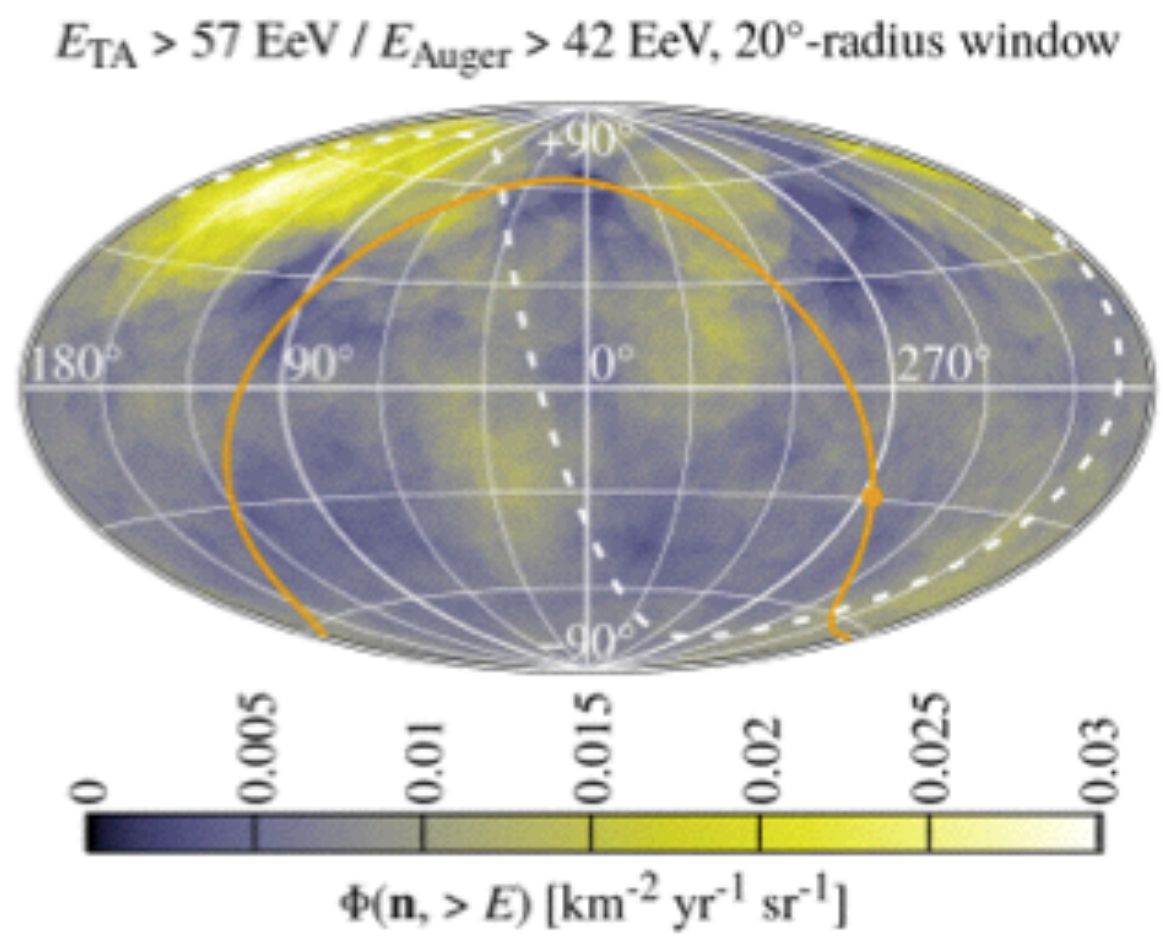

Summary and perspectives

- Ultimate goal: full-sky survey of UHECR patterns in the sky
  - Large scale studies >~10 EeV (beyond the dipole)
  - Over-densities/correlations with xGal matter at UHE

E_{TA}>10 EeV / E_{Auger}>8.5 EeV

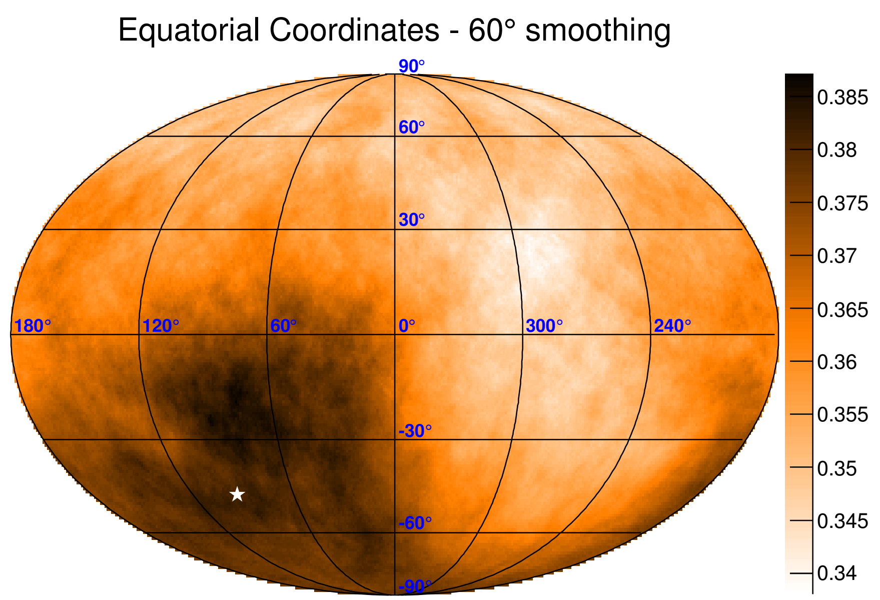

ApJ 794 (2014) 172

E_{TA} > 57 EeV / E_{Auger} > 42 EeV, 20°-radius window

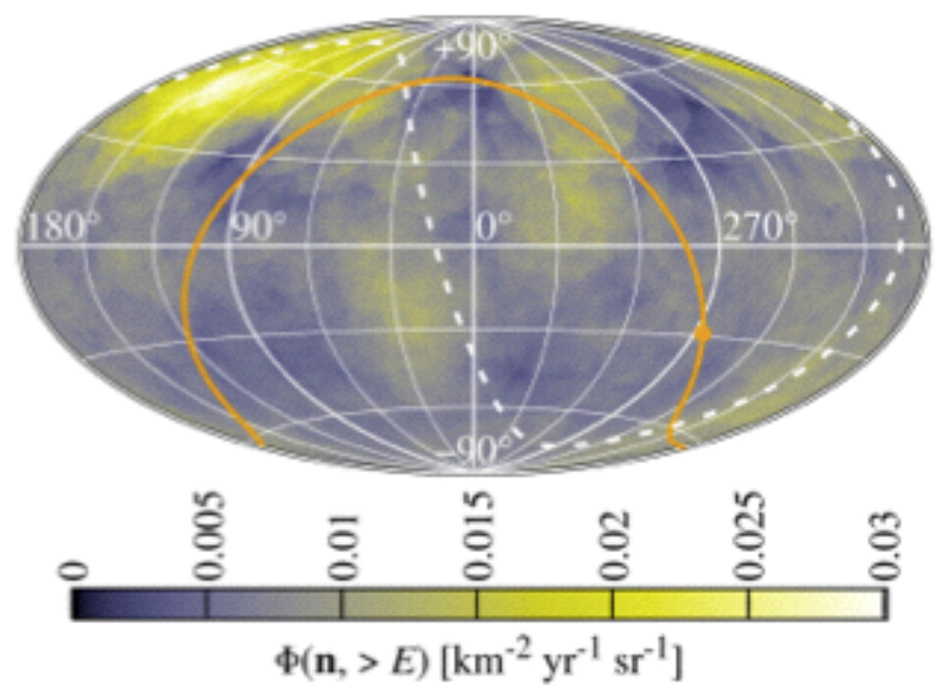

A. Di Matteo, UHECR2016

Extragalactic gamma-ray background

Extragalactic γ-ray background dominated by 2 types of sources:

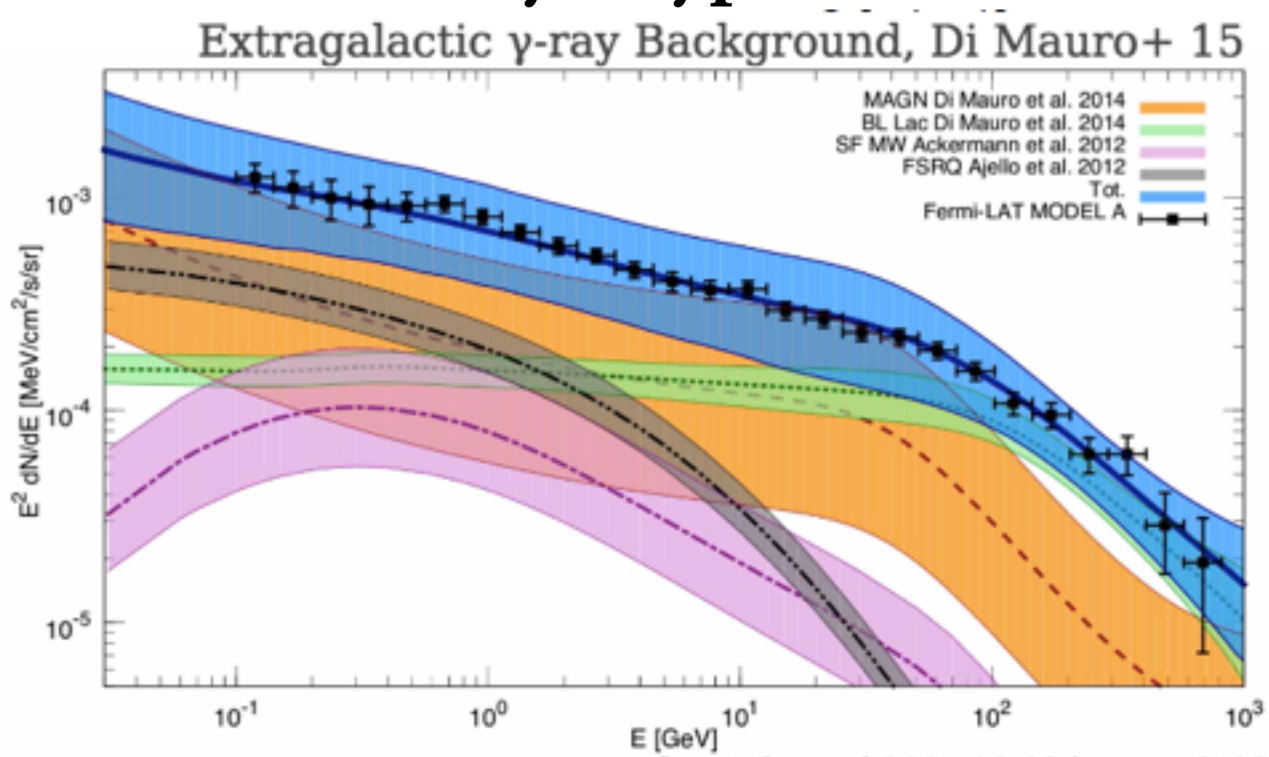

- γAGNs: For a jet with a relativistic bulk motion, UHECRs emitted isotropically in the bulk frame would appear to be coming out in the jet direction in our cosmic reference frame.
- SBGs: high gamma-ray luminosity thought to be due to intense starburst episodes possibly triggered by galaxy mergers; could harbor with an increased rate cataclysmic events associated with the deaths of short-lived, massive stars, such as gamma-ray bursts, hypernovæ, and magnetars

UHECR source candidates: requirement on power

- >1 EeV, energy production rate close to 10^{45} erg Mpc^{-3} yr^{-1}
- Both local SBGs & γAGNs match this requirement

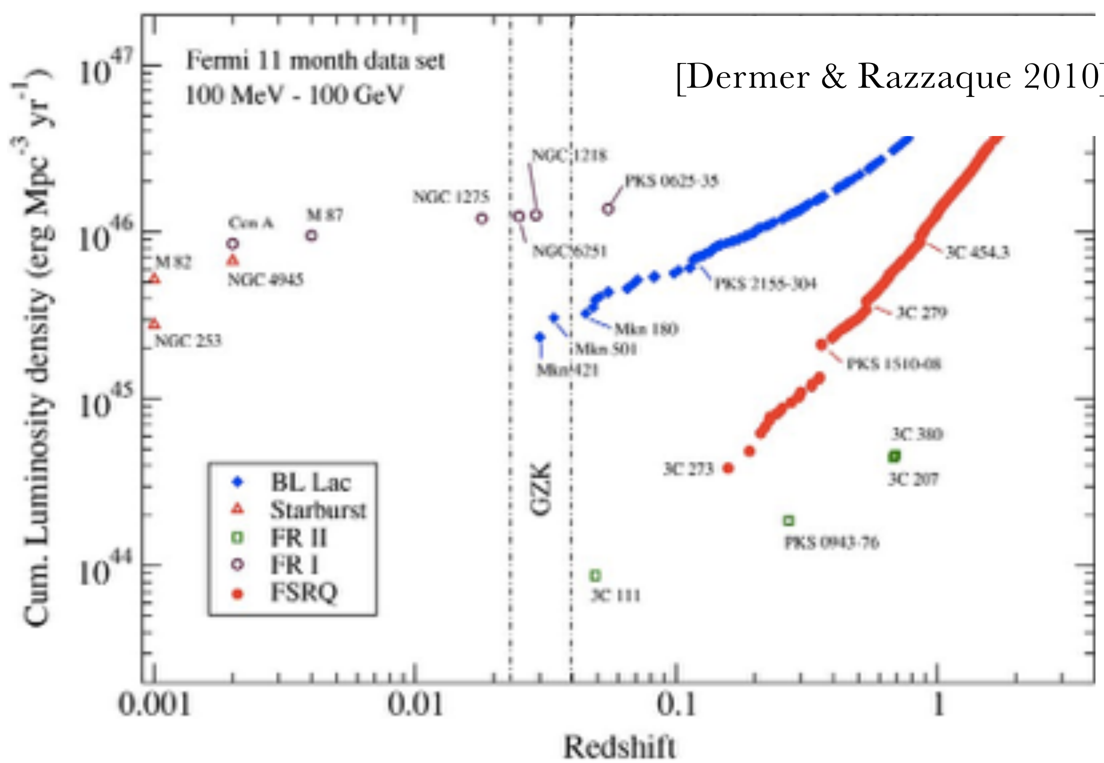

Catalog of star-forming galaxies

GeV—TeV observations

- **TeV**: M 82 (0.9% Crab), NGC 253 (0.2% Crab), NGC 4945 ⊘, NGC 1068 (<5%), M 83 (<2%)
- **GeV**: M 82, NGC 253, NCG 4945, NGC 1068 firmly detected. GeV/FIR/radio correlation

➡ Flux at 1.4 GHz used as a **proxy** for the UHECR flux

Credits: Q. Luce (IPNO)

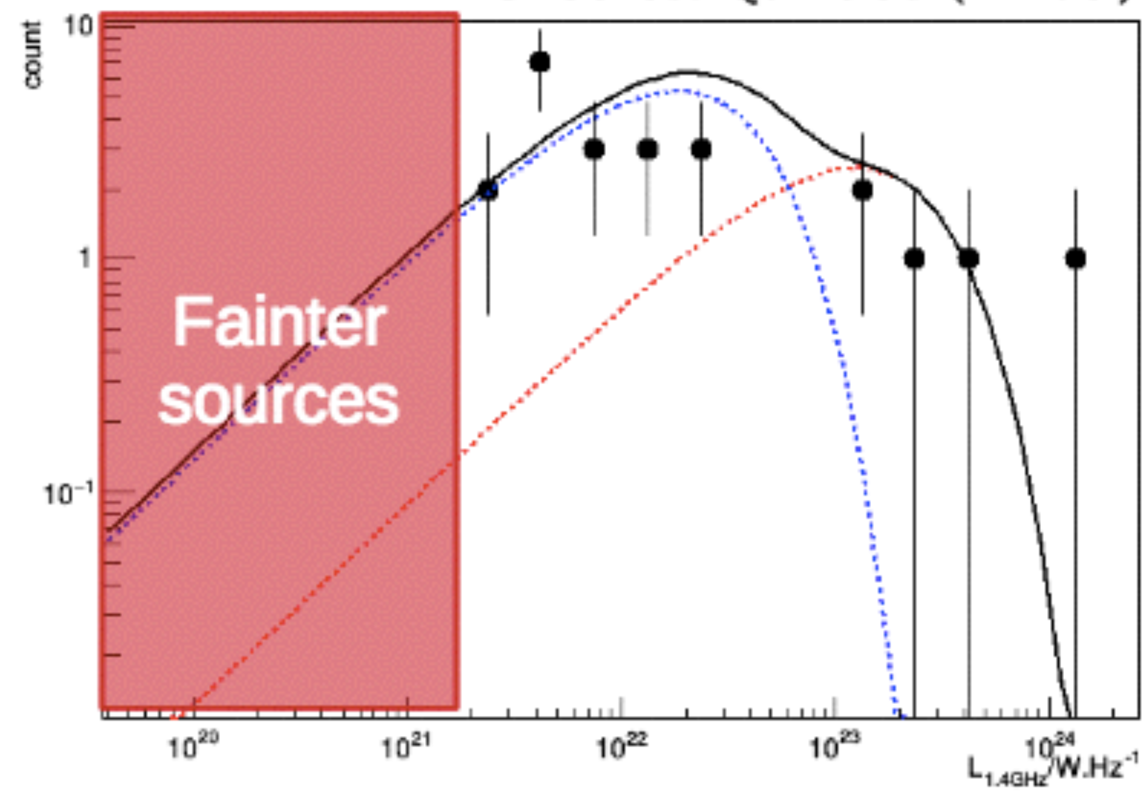

Model Flux Map - Starburst galaxies - E > 39 EeV

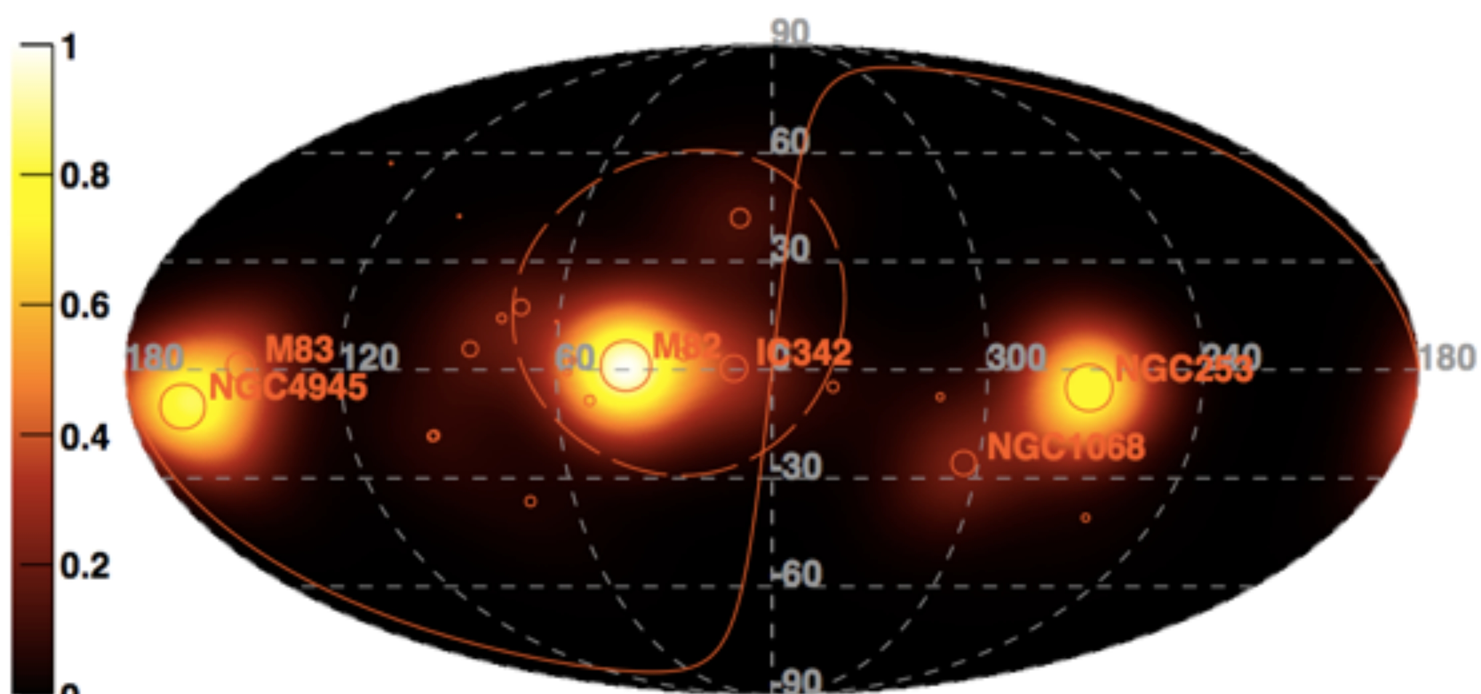

supergalactic coordinates

Selected catalog

- ApJ 755, 164 (2012)
- Cut @ 0.3 Jy to maximize the completeness
- Cut that matches a ~200 Mpc GZK horizon: take the most luminous source in the sample, place it as far away as you can to detect it above 0.3 Jy → 173 Mpc
- 23 brightest (/63) — ~80% of total flux

Control of the event rate

- Auger: Full efficiency of detection above 3 EeV
- But effective change of rate due to changes of atm. conditions

- **Energies corrected by atmospheric changes for θ < 60º**
  - Air-density ⟶ lateral distribution of EM component
  - Pressure ⟶ longitudinal depth of observation

Induces modulations of ±1.7% in solar frequency

[Auger Coll. JINST 12 (2017) P02006]

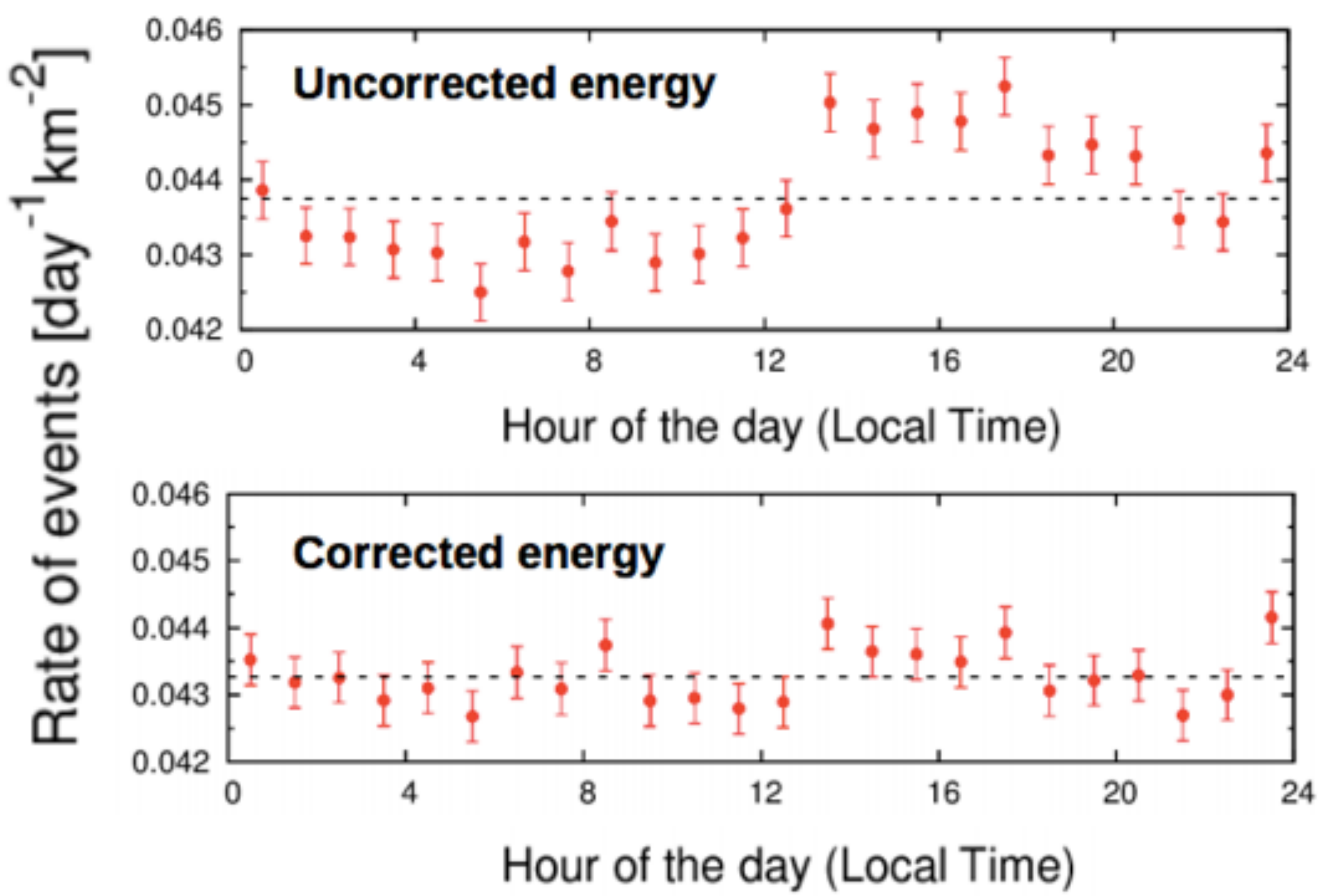

$$E_{\mathrm{grd}} = (1+\eta(t))E$$

$$I(E_{\mathrm{grd}})\mathrm{d}E_{\mathrm{grd}} = I(E)\mathrm{d}E = KE^{-\gamma}\mathrm{d}E$$

➡ Variations prop. to $1+(\gamma-1)\eta(t)$.

Stationarity? example #1

✓ Stationarity: example #1

$$\tilde{C}_\ell = \frac{1}{2\ell+1}\sum_{m=-\ell}^{m=\ell} |\tilde{a}_{\ell m}|^2$$

Stationarity? example #2

$$\tilde{C}_\ell = \frac{1}{2\ell+1}\sum_{m=-\ell}^{m=\ell} |\tilde{a}_{\ell m}|^2$$

Stationarity? example #2

$$\tilde{C}_\ell = \frac{1}{2\ell+1} \sum_{m=-\ell}^{m=\ell} |\tilde{a}_{\ell m}|^2$$

?

✗ Stationarity: example #2